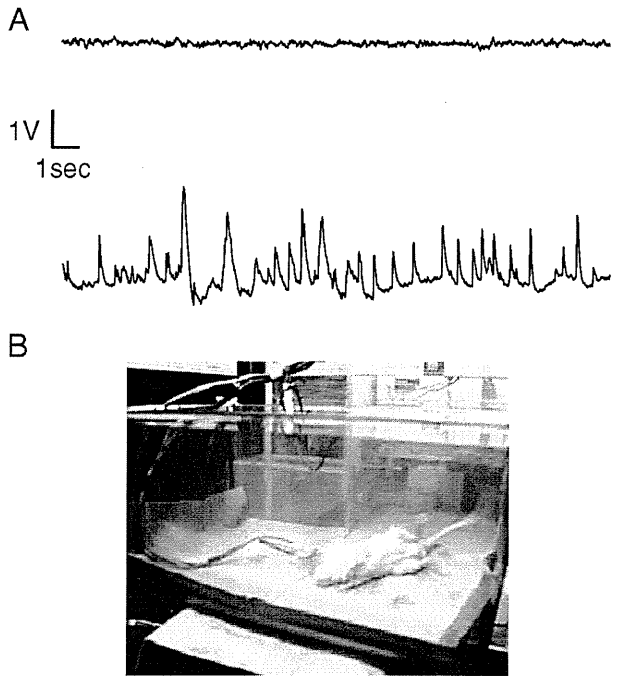

Fig. 5 – Cortical EEG recording in ADMS rat by cold-swim tests. (A) EEG recorded from an ADMS rat before the test (upper) and during the cold-swim induced clonus behaviour (lower). (B) A photograph shows characteristic posture during the clonus behaviour.

swimming, showing head shaking and twitching behaviour in the water. When removed from the water, ADMS rats exhibited severe neuromyotonia (Supplementary Video 4) and tremors, with the eyes shut and whiskers flickering. After a few minutes of tremors lasting, and even worsening, the rats demonstrated head nodding, forelimb clonus and rearing. Cortical EEG recordings showed aberrant spike-and-wave discharges (2-3 Hz) associated with clonus behaviours (Figs. 5A, B). The tremors and clonus phenotypes were reduced as time progressed, but when the animals started to walk, its movements were staggering and ataxic (Supplementary Video 5). Normal behaviour was fully recovered after 20 min. Cold-swim induced tremors, neuromyotonia, clonus, and motor incoordination, were present in all ADMS rats tested (n=7). In contrast, none of the behaviours was observed in WT rats (n=5).

2.7. *Electrophysiological properties of S309T channel*

To investigate the functional consequences of the S309T mutation on the Kv1.1 channel, we transfected HEK 293 cells with *Kcna1* cDNA (WT or S309T) and recorded whole-cell current responses. At a holding potential of −80 mV, current families were obtained by sequential 100-ms depolarizing commands from −100 to 50 mV, delivered in 10 mV increments. Typical delayed-rectifier potassium currents were recorded from cells expressing Kv1.1 WT, whereas minimal currents were detected from cells expressing Kv1.1 S309T or from mock-transfected cells (Figs. 6A, B). In western blot analysis, a single 56-kD band was detected in cells transfected with *Kcna1* WT or S309T cDNA (Fig. 6C). To investigate whether the S309T mutation has an effect on the intracellular trafficking of Kv1.1, we analysed the cell-surface expression of Kv1.1, by biotinylating the surface proteins on HEK cells. Precipitation of the solubilized biotinylated proteins with streptavidin beads, followed by western blotting, detected expression of both WT and S309T variants of Kv1.1 on the cell surface (Fig. 6D).

Because ADMS rats carrying the *Kcna1* S309T mutation dominantly display several neurological abnormalities, the opening of Kv1.1 channels may be disturbed when one or more S309T-containing subunits are incorporated into the tetrameric complex of Kv1.1 channels. To test this hypothesis, we co-injected cRNAs for WT and S309T mutant subunits in *Xenopus* oocytes, and measured current responses under a two electrode voltage clamp configuration. At a holding potential of −60 mV, current families were obtained by 500-ms depolarizing commands (with a 500 ms prepulse at −120 mV) from −60 to 60 mV, delivered in 20 mV increments. The co-injection of WT and S309T cRNA (1:1 ratio) resulted in reduced outward currents, with an approximately 80% smaller amplitude than that of WT-injected oocytes at 0 mV, suggesting a dominant-negative effect of the S309T subunit on the function of heterotetrameric Kv1.1 channels (Figs. 6E, F). Western blot analysis showed equivalent Kv1.1 protein expression levels among the three groups (WT, S309T and WT:S309T (1:1) co-injected) of oocytes (Fig. 6G).

3. Discussion

Table 1 summarizes the *Kcna1*-mutant animal models for EA1 previously reported in mice and rats. They exhibit diverse neurological phenotypes and show differing functional defects of the potassium channel, Kv1.1 (Herson et al., 2003; Petersson et al., 2003; Smart et al., 1998). *Kcna1*-knockout mice have a complete deletion of *Kcna1*, and have enormously contributed to our fundamental understanding of Kv1.1 function (Glasscock et al., 2010; Kopp-Scheinpflug et al., 2003; Lopantsev et al., 2003; Smart et al., 1998; Zhang et al., 1999; Zhou et al., 1998). Homozygous *Kcna1*-knockout mice exhibit various neurological defects, namely, spontaneous seizure activities associated with elevated excitability of the hippocampal CA3 neurons (Lopantsev et al., 2003), and/or of the auditory neurons of the medial nucleus of the trapezoid body (MNTB) (Kopp-Scheinpflug et al., 2003). Other defects include temperature-sensitive nerve excitability in the PNS (Zhou et al., 1998), alteration of GABAergic inhibition in cerebellar Purkinje cells (Zhang et al., 1999), and premature death potentially associated with cardiac dysfunction (Glasscock et al., 2010). However, to date, no mutation causing a complete deletion of the *KCNA1* gene has been reported in human EA1. Spontaneous mutant mice, *megencephaly*, expressing a truncated KCNA1 protein of 230 residues, recessively exhibit progressive brain overgrowth and epileptic behaviours similar to knockout mice (Persson et al., 2005; Petersson et al., 2003). *Kcna1*-knockin mice induced by the V408A EA1 mutation, show stress-induced loss of motor coordination, which mimics the symptoms of human EA1 (Herson et al., 2003). However, none of the mouse models shows spontaneous behavioural

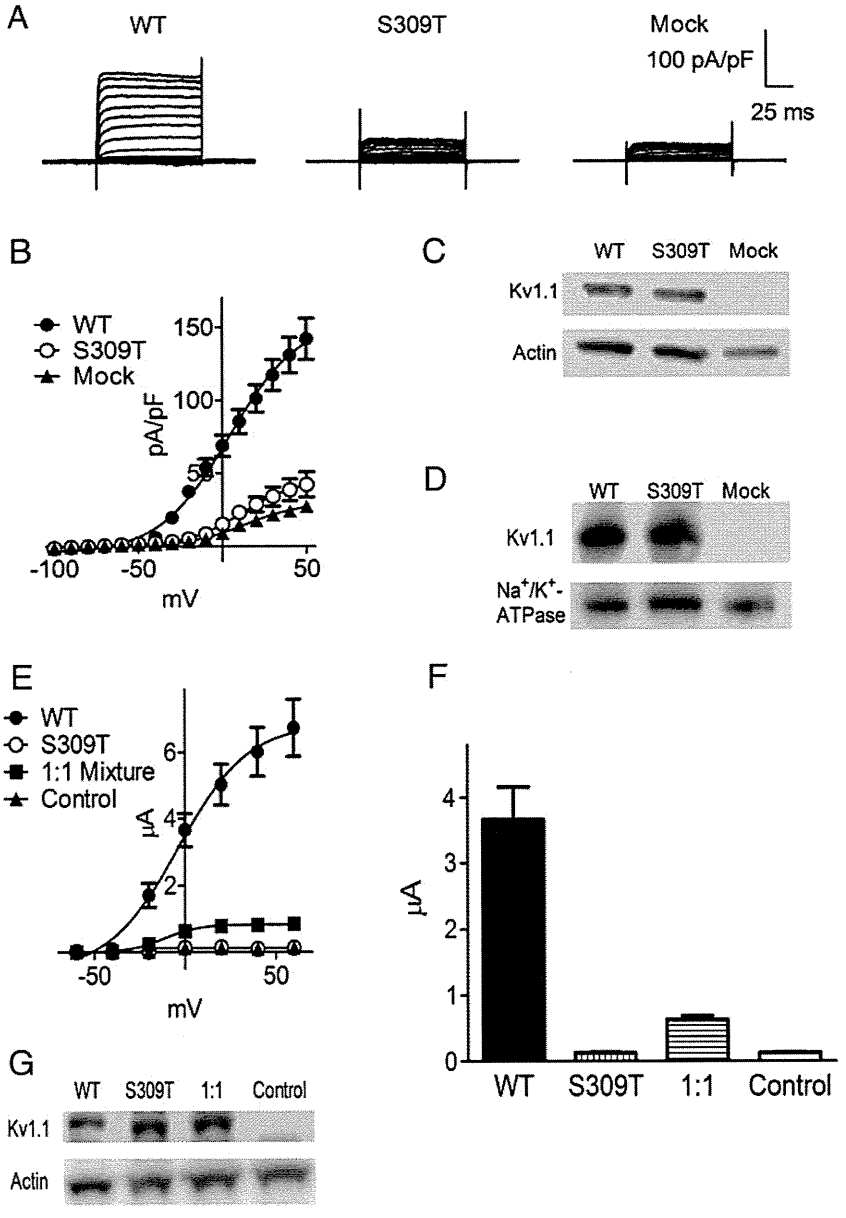

Fig. 6 – Electrophysiological properties of S309T channel. (A) Typical whole-cell current families recorded from HEK 293 cells transfected with cDNAs encoding Kv1.1 WT (left), S309T (centre) and transfection control (mock, right). Minimal currents were detected from cells expressing Kv1.1 S309T or from mock-transfected cells. (B) I–V relationships of Kv1.1 channels recorded from HEK cells transfected with each variant (n=4–5). (C, D) Western blot analysis of (C) whole cell lysate and (D) cell surface fractions of HEK cells transfected with each variant. Both WT and S309T Kv1.1 proteins were expressed on the cell surface. (E) I–V relationships of Kv1.1 channels recorded from *Xenopus* oocytes injected with WT cRNA, S309T cRNA and 1:1 mixture of WT and S309T cRNAs (n=4). The total amount of injected cRNAs was adjusted to 5 ng/oocyte. (F) Current amplitude recorded in response to 0 mV voltage pulse shown in (E). The co-injection of WT and S309T cRNA resulted in 80% smaller currents than WT-injected oocytes. (G) Western blot analysis indicated equivalent Kv1.1 protein expression levels among the three groups of cRNA injected oocytes, WT, S309T and WT:S309T (1:1) co-injected.

phenotypes in heterozygotes, in contrast to the ADMS rats, which we have shown to dominantly express convulsive seizures, myokymia and neuromyotonia. These neurological phenotypes are similar to symptoms of human EA1, and are severe compared with current mouse models. Interestingly, as far as we know, the myokymia phenotype detected by EMG recording in ADMS rats, has not been reported in any of the mouse models, but is always detected in individuals with human EA1. Considering EA1 patients exhibiting myokymia in the limbs or especially in the muscles of the face or the hands (Pessia and Hanna, 1993), myokymia with a predilection for forelimbs of ADMS rats may partially mimic the EA1 symptoms of human patients.

What mechanism is responsible for the phenotypic differences between the EA1 models? Strain-dependent genetic

Table 1 – Phenotype comparison of *Kcna1* mutant animals and relevance as EA1 models.

Animals	Mutation		Phenotypes				Protein functions in vitro		
			Lethality	Seizure (CNS)	Myokymia, neuromyotonia (PNS)	Episodic ataxia (cerebellum)	Channel activity	Expression, trafficking	Tetrameric channels
Kcna1 knockout mice (Smart et al., 1998)	Null	Hetero	–	± susceptible to flurothyl-induced seizures	–	–	↓↓↓ no activity	↓ half expression	–
		Homo	~50% die until 5 weeks	+++ spontaneous seizures start from 3–4 weeks	± cold-swim induced tremor and neuromyotonia	± cold-swim induced motor incoordination		↓↓↓ no expression	
megencephaly mice (Petersson et al., 2003)	Truncation at 230aa	Hetero	- (increased brain volume)	–	–	–	↓↓↓ no activity	–	Forming tetramers, impeded?
		Homo		+++ spontaneous seizures start from 5–6 weeks	+ startle responses	+ shakiness in gait		↓↓↓ trapped in endoplasmic reticulum	
V408A knockin mice (Herson et al., 2003)	Missense V408A	Hetero	–	–	–	± isoproterenol-induced motor incoordination	↓↓ reduced current, slow inactivation	Normal expression and trafficking	Interrupting WT-Kv1.1 channels
		Homo	embryonic lethal at E3-E9	–	–	–			
ADMS S309T rats	Missense S309T	Hetero	~80% die until 30 weeks	+++ spontaneous seizures start from 12–14 weeks	+++ myokymia, neuromyotonia, startle responses	± cold-swim induced motor incoordination	↓↓↓ no current	Normal expression and trafficking	Interrupting WT-Kv1.1 channels
		Homo	postnatal lethal at P10–P18	++++ spontaneous seizures start from P10	++++ extension of hind limbs, tremor	+++ ataxia			

background or species differences between mouse and rat likely play a part. Seizure onset was delayed or even prevented in F1 and BC1 progeny of BN rats, suggesting the influence of modifier gene(s). In human EA1, neuromyotonia is generally associated with KCNA1 mutations; conversely, epilepsy is not associated with mutations in potassium channels, but with other factors such as modifier genes (Pessia and Hanna, 1993; Poujois et al., 2006; Rajakulendran et al., 2007; Zuberi et al., 1999). In mice, impaired Ca^{2+}-channel function as a result of *Cacna1a* mutations, show improved seizure susceptibility by altering neuronal network excitability in *Kcna1*-knockout mice, demonstrating protective interactions between ion channel variants (Glasscock et al., 2007). A further interaction between *Kcna1* and another gene, *Lgi1*, was implicated in a rare autosomal dominant form of temporal lobe epilepsy, and shown to modulate fast inactivation of Kv1.1 (Schulte et al., 2006). Further genetic analysis focusing on seizure susceptibility in the (ADMS×BN)×BN backcross progeny may offer insights into the modifier gene(s) associated with seizure onset.

The distinct mutations of *Kcna1* may explain the wide variety of clinical phenotypes in EA1. Our expression studies of homomeric S309T Kv1.1 channels in HEK cells indicated cell-surface expression of the channels is non-functional in terms of their biophysical properties (Fig. 6). Heteromeric expression of S309T and WT Kv1.1 channels in *Xenopus* oocytes resulted in greatly reduced currents compared with WT Kv1.1 channels, suggesting the S309T mutation has a dominant-negative effect on the potassium channel, consistent with previous functional studies on EA1 mutations (Chen et al., 2007; D'Adamo et al., 1999; Imbrici et al., 2011; Zuberi et al., 1999). The *mceph* truncated protein, containing only the N-terminal domain, is retained in the endoplasmic reticulum and not expressed on the cell surface (Persson et al., 2005) (Table 1). On the other hand, V408A Kv1.1 channels show normal cell-surface expression and partially reduced potassium currents (Adelman et al., 1995). It was also reported that the V408A Kv1.1 channels reduce the rate of inactivation by a decreased affinity for the N-terminal inactivation domain of co-assembled WT Kv1.1 in heterotetramers, which could explain the dominant-negative effects of the V408A Kv1.1 channels (Imbrici et al., 2011). T226K Kv1.1 channels in EA1 also showed a dominant-negative effect when co-expressed in oocytes with the WT Kv1.1 (Chen et al., 2007). In addition, Kv1.1-containing channels in the mammalian central nervous system co-assembled with Kv1.2 and Kv1.4 subunits, which may be also interrupted by the cell-surface expressed mutated Kv1.1 subunit in heterotetramers (D'Adamo et al., 1999; Imbrici et al., 2006). The dominant-negative effects of the V408A Kv1.1 channels in knockin mice as well as S309T Kv1.1 channels in ADMS rats may explain the lethality of the homozygous animals, which are different from that of knockout and *mceph* mice.

In conclusion, using an ENU mutagenesis approach, we have generated *Kcna1*-mutant rats that dominantly express persistent myokymia, neuromyotonia, stress-induced motor incoordination and spontaneous convulsive seizures, as the first rat model of human EA1. The ADMS rat provides a useful animal model of human EA1 to understand the underlying mechanisms of the various clinical phenotypes of *KCNA1*-associated diseases.

4. Experimental procedures

4.1. *Rats and ENU mutagenesis*

Male F344/NSlc (F344) rats (Japan SLC, Hamamatsu, Japan) received two intraperitoneal (i.p.) injections of the chemical mutagen ENU (40 mg/kg) as previously described (Mashimo et al., 2008). Ten weeks after the second ENU injection, males were bred to untreated F344 females to generate ENU-mutagenized G1 progeny (mean mutation frequency: approximately 1 in 4 million base pairs). One female exhibiting muscle twitching and epileptic seizures, was identified and classified as an "affected" founder, then backcrossed to a F344 background, for ten generations (N2–N10), to remove latent ENU-induced mutations in other chromosomal regions. Heterozygous affected N10 males and females were intercrossed to generate the homozygous mutation.

The animal care and experimental procedures used were approved by the Animal Research Committee, Kyoto University and carried out according to the Regulation on Animal Experimentation at Kyoto University. The ADMS rat has been deposited into the National Bio Resource Project — Rat in Japan (NBPR-Rat No. 0458) and is available from the Project (http://www.anim.med.kyoto-u.ac.jp/nbr).

4.2. *Electromyography (EMG) recording*

Rats at 16 weeks of age were used for electromyography (EMG) recordings from muscles in the forelimb (musculus triceps brachii) and hindlimb (musculus quadriceps femoris). To implant EMG electrodes, rats were anesthetized with pentobarbital sodium (50 mg/kg i.p.). Enamel-coated stainless-steel electrodes (100 μm diameter), were prepared by flexing the electrode into a hair-pin curve, 5 mm from the distal end of the electrode. Electrodes were then hooked onto the bevel edge of a 23 gauge injection needle and inserted into the muscle through the overlying skin. The injection needle was removed, leaving the electrode implanted in the appropriate muscle. Pairs of electrodes were implanted in each muscle, to allow bipolar recording, and a ground electrode was inserted subcutaneously on the back. After recovery from anaesthesia, EMG activity was recorded under freely moving conditions, and combined with behavioural observations made using an amplifier (MEG-6108; Nihon Kohden, Tokyo, Japan) and a thermal alley recorder (RTA-1100; Nihon Kohden). The recorded signals were stored (PowerLab ML845; AD Instruments, Bella Vista, Australia) for analysis.

4.3. *Electroencephalogram (EEG) recording*

Rats at 10–20 weeks of age were anesthetized with pentobarbital sodium (50 mg/kg i.p.), and fixed in a stereotaxic instrument (David Kopf Instruments, Tujunga, USA) for implantation of EEG electrodes. Small holes were made in the skull, and screw electrodes were placed on the surface of the right frontal cortex. Enamel-coated stainless-steel electrodes were implanted in the hippocampus (3.8 mm caudal and 2.0 mm lateral to the bregma, and 2.2 mm from the cortex surface). A reference electrode was implanted on the left frontal cranium. The electrodes were then connected to a miniature plug and fixed to the skull with dental cement. After a 1-week recovery period, animals

with chronically implanted electrodes were placed in a shielded box ($40 \times 40 \times 40$ cm^3). Under freely moving conditions, continuous EEG recordings were made for 3 h during daytime (light-on), with behavioural observations made using an amplifier (MEG-6108; Nihon Kohden) and a thermal alley recorder (RTA-1100; Nihon Kohden). The recorded signals were stored (PowerLab ML845; AD Instruments) for analysis.

4.4. *Antiepileptic drug testing*

Carbamazepine (Sigma-Aldrich Co., St. Louis, USA) dissolved in polyethylene glycol 400 (PEG 400) was used for drug testing (20 mg/kg i.p.), or saline solution (1 ml/kg i.p.) as control. Five ADMS rats at 16–19 weeks of age were observed for 3 h during daytime (light-on) from 30 min after the administration.

4.5. *Histopathology*

Rats at 16–19 weeks of age were deeply anesthetized with sodium pentobarbital (50 mg/kg i.p.). Brains were removed, post-fixed in Bouin's fixative and paraffin embedded. 4 μm paraffin sections were cut and stained with haematoxylin and eosin to evaluate morphological changes.

4.6. *Genetic mapping of Adms*

We produced a total of 180 (BN/SsNSlc × ADMS) × BN/SsNSlc backcross progeny. Genotyping for the *Adms* locus was performed in rats that exhibited the twitching phenotype at 10–14 weeks of age, since spontaneous seizures were not observed in the backcross progeny until at least 20 weeks of age. To localize the *Adms* locus to a specific chromosomal region, we performed genome-wide scanning on DNA samples using a panel of 121 simple sequence length polymorphism (SSLP) markers that cover all the autosomal chromosomes (Chrs). Genomic DNA was prepared from tail biopsies using an automatic DNA purification system (PI-200; Kurabo, Osaka, Japan). All PCRs were performed for 35 cycles (denaturation at 94 °C for 30 s, annealing at 60 °C for 1 min, and extension at 72 °C for 45 s), using Taq polymerase (Takara Bio, Otsu, Japan). PCR products were examined on 4% agarose gels with ethidium bromide staining.

4.7. *Sequence analysis*

The primers used for sequencing the coding regions of *Kcna1*, *Kcna5*, and *Kcna6* are described in Supplementary Table 1. PCR products from genomic DNA were reacted with BigDye Terminator v3.1 cycle sequencing mix (Applied Biosystems, Foster City, USA), followed by the standard protocol for the Applied Biosystems 3100 DNA Sequencer.

4.8. *Western blotting*

Protein lysates were prepared from P10 rat brain as previously described (Imai et al., 2007). 25 μg of each sample was separated on 10% Bis–Tris polyacrylamide gels and analysed by western blotting using rat KCNA1 (ab32433; Abcam, Cambridge, UK) and β-actin (AC-40; Sigma Aldrich) primary antibodies. Secondary antibodies against rabbit IgG (NA934; GE Healthcare Bio-Sciences, Little Chalfont, UK) and mouse IgG (NA931; GE Healthcare Biosciences) were used, respectively.

4.9. *Swimming tests*

Rats at 5 weeks of age were placed in the middle of a tank (30 cm × 60 cm, filled with water to a depth of 20 cm) to swim. The water temperature was 17 or 38 °C, and the swim time was 2 min. After swimming, the rats were placed on a dry platform (room temperature 24 °C) for behavioural observation.

4.10. *Cell culture and transfection*

Rat *Kcna1* is encoded by a single exon, allowing the coding region of wild-type (WT) or S309T mutant *Kcna1* to be PCR amplified from genomic DNA. PCR products were inserted into pGEM-T Easy (Promega, Fitchburg, USA) and sequenced to confirm the presence of the S309T mutation. The full length cDNA for each variant (*Kcna1* WT or S309T), was subcloned into pcDNA3.1(–) (Invitrogen, Carlsbad, USA), for western blot analysis, and pIRES2-EGFP (Clontech, Mountain View, USA) for current recording. mRNA was transcribed in vitro using T7-RNA polymerase and a High Yield Capped RNA transcription kit (EPICENTRE Biotechnologies, Madison, USA).

Human embryonic kidney (HEK) 293 cells were grown to 80% confluence in Dulbecco's modified Eagle's medium supplemented with 10% foetal bovine serum, 50 U/ml penicillin and 50 μg/ml streptomycin at 37 °C. Cells were transfected with Lipofectamine 2000 (Invitrogen). For western blot analysis, cells were transfected with pcDNA3.1(–) containing *Kcna1* WT or S309T cDNAs, and maintained for 24 h before harvesting. For whole-cell current recording, cells were transfected with pIRES2-EGFP containing *Kcna1* WT or S309T cDNAs, then plated on glass coverslips at 10% confluence 24 h after transfection, and maintained for another 24 h.

4.11. *Cell-surface biotinylation*

24 h after transfection, HEK 293 cells in 35 mm tissue culture dishes were washed with PBS-CM (PBS containing 1 mM $MgCl_2$ and 0.1 mM $CaCl_2$), then incubated in 0.8 ml of EZ-Link Sulfo-NHS-biotin solution (1 mg/ml in PBS-CM; Thermo Scientific, Waltham, USA) for 30 min on ice. After washing with ice-cold quenching solution (PBS-CM containing 100 mM glycine), cells were incubated in 1 mL quenching solution for 45 min at 4 °C before harvesting, followed by centrifugation for 6 min at $6000 \times g$. Cells were then solubilized on ice in 300 μl RIPA buffer (1% Triton X-100, 0.1% SDS, 150 mM NaCl, 1 mM EDTA and 50 mM Tris, pH 7.5 with HCl) containing 1% protease inhibitor cocktail (Invitrogen). The resulting cell lysate was centrifuged for 20 min at $14000 \times g$, and the supernatant collected. UltraLink® immobilized streptavidin (Thermo Scientific) was added to the supernatant at a ratio of 1:6, and then incubated overnight at 4 °C with agitation. Next, samples were centrifuged for 1 min at $5000 \times g$, and the resin washed with RIPA buffer, high-salt buffer (0.1% Triton X-100, 500 mM NaCl, 5 mM EDTA, 50 mM Tris, pH 7.4 with HCl), and 50 mM Tris (pH7.4 with HCl). Proteins were eluted from the resin by the addition of LDS sample buffer (Invitrogen).

4.12. *Electrophysiological recording from HEK 293 cells*

Whole-cell currents were recorded at room temperature with an EPC 9 amplifier (HEKA, Lambrecht, Germany). Currents were sampled and analysed with Patchmaster 2.43 software (HEKA). Patch pipettes were made from borosilicate glass capillaries (1.5-mm outer diameter; Narishige, Tokyo, Japan) using a P-87 micropipette puller (Sutter Instruments, Novato, USA). The resistance ranged from 2 to 4 MΩ when filled with pipette solution (138 mM NaCl, 5.4 mM KCl, 1.2 mM $MgCl_2$, 1 mM $CaCl_2$, 10 mM EGTA, 10 mM HEPES, 10 mM glucose, pH 7.3 with NaOH). The recording solution was 138 mM NaCl, 5.4 mM KCl, 1.2 mM $MgCl_2$, 1 mM $CaCl_2$, 10 mM EGTA, 10 mM HEPES, 10 mM glucose, pH 7.3 with NaOH.

4.13. *Electrophysiological recording from* **Xenopus** *oocytes*

Small pieces of ovary were isolated from cold-anesthetized *Xenopus laevis* and incubated in Ca^{2+}-free solution (88 mM NaCl, 1 mM KCl, 0.82 mM $MgSO_4$, 2.4 mM $NaHCO_3$, 7.5 mM Tris, pH 7.4 with HCl), containing 1.5 mg/ml collagenase (Sigma-Aldrich) at 20 °C for 3 h. Stage V and VI oocytes were selected and injected with 25 nl of cRNA solution for each *Kcna1* variant (WT or S309T). The injected oocytes were maintained at 20 °C for 4 days in modified Barth's solution (88 mM NaCl, 1 mM KCl, 0.41 mM $CaCl_2$, 0.33 mM $Ca(NO_3)_2$, 0.82 mM $MgSO_4$, 2.4 mM $NaHCO_3$, 7.5 mM Tris, pH7.4 with HCl), supplemented with 300 μg/ml sodium pyruvate, 10 U/ml penicillin and 10 μg/ml streptomycin. Currents were recorded at 20 °C with an OC-725C amplifier (Warner Instruments, Hamden, USA). Currents were sampled and analysed with a PowerLab 2/25 system (AD Instruments) and Scope 4.0.7 software (AD Instruments). The injected oocytes were voltage-clamped at a holding potential of −60 mV with two intracellular glass electrodes (1–2 MΩ with 3 M KCl), made from borosilicate glass capillaries (1.5-mm outer diameter; Narishige) using a PE-2 puller (Narishige). The recording solution was 115 mM NaCl, 2 mM KCl, 2 mM $CaCl_2$, 2 mM $MgCl_2$, 10 mM HEPES, pH 7.2 with NaOH.

Supplementary materials related to this article can be found online at doi:10.1016/j.brainres.2011.11.023.

Acknowledgments

This work was supported in part by Grant-in-Aid for Scientific Research from the Ministry of Education, Culture, Sports, Science and Technology (16200029 to T.M.); and Industrial Technology Research Grant Program from the New Energy and Industrial Technology Development Organization of Japan (08A02004a to T.M.). We would like to thank Fumi Tagami and Yayoi Kunihiro for technical help, and Masashi Sasa for his helpful consultations.

REFERENCES

Adelman, J.P., Bond, C.T., Pessia, M., Maylie, J., 1995. Episodic ataxia results from voltage-dependent potassium channels with altered functions. Neuron 15, 1449–1454.

Bretschneider, F., Wrisch, A., Lehmann-Horn, F., Grissmer, S., 1999. Expression in mammalian cells and electrophysiological characterization of two mutant Kv1.1 channels causing episodic ataxia type 1 (EA-1). Eur. J. Neurosci. 11, 2403–2412.

Browne, D.L., Gancher, S.T., Nutt, J.G., Brunt, E.R., Smith, E.A., Kramer, P., Litt, M., 1994. Episodic ataxia/myokymia syndrome is associated with point mutations in the human potassium channel gene, KCNA1. Nat. Genet. 8, 136–140.

Browne, D.L., Brunt, E.R., Griggs, R.C., Nutt, J.G., Gancher, S.T., Smith, E.A., Litt, M., 1995. Identification of two new KCNA1 mutations in episodic ataxia/myokymia families. Hum. Mol. Genet. 4, 1671–1672.

Chen, H., von Hehn, C., Kaczmarek, L.K., Ment, L.R., Pober, B.R., Hisama, F.M., 2007. Functional analysis of a novel potassium channel (KCNA1) mutation in hereditary myokymia. Neurogenetics 8, 131–135.

Comu, S., Giuliani, M., Narayanan, V., 1996. Episodic ataxia and myokymia syndrome: a new mutation of potassium channel gene Kv1.1. Ann. Neurol. 40, 684–687.

D'Adamo, M.C., Imbrici, P., Sponcichetti, F., Pessia, M., 1999. Mutations in the KCNA1 gene associated with episodic ataxia type-1 syndrome impair heteromeric voltage-gated K(+) channel function. FASEB J. 13, 1335–1345.

Demos, M.K., Macri, V., Farrell, K., Nelson, T.N., Chapman, K., Accili, E., Armstrong, L., 2009. A novel KCNA1 mutation associated with global delay and persistent cerebellar dysfunction. Mov. Disord. 24, 778–782.

Eunson, L.H., Rea, R., Zuberi, S.M., Youroukos, S., Panayiotopoulos, C.P., Liguori, R., Avoni, P., McWilliam, R.C., Stephenson, J.B., Hanna, M.G., Kullmann, D.M., Spauschus, A., 2000. Clinical, genetic, and expression studies of mutations in the potassium channel gene KCNA1 reveal new phenotypic variability. Ann. Neurol. 48, 647–656.

Gilbert, G.J., Graves, T.D., Kullmann, D.M., 2011. Nongenetic factors influence severity of episodic ataxia type 1 in monozygotic twins. Neurology 76, 490 (author reply 490).

Glasscock, E., Qian, J., Yoo, J.W., Noebels, J.L., 2007. Masking epilepsy by combining two epilepsy genes. Nat. Neurosci. 10, 1554–1558.

Glasscock, E., Yoo, J.W., Chen, T.T., Klassen, T.L., Noebels, J.L., 2010. Kv1.1 potassium channel deficiency reveals brain-driven cardiac dysfunction as a candidate mechanism for sudden unexplained death in epilepsy. J. Neurosci. 30, 5167–5175.

Glaudemans, B., van der Wijst, J., Scola, R.H., Lorenzoni, P.J., Heister, A., van der Kemp, A.W., Knoers, N.V., Hoenderop, J.G., Bindels, R.J., 2009a. A missense mutation in the Kv1.1 voltage-gated potassium channel-encoding gene KCNA1 is linked to human autosomal dominant hypomagnesemia. J. Clin. Invest. 119, 936–942.

Glaudemans, B., van der Wijst, J., Scola, R.H., Lorenzoni, P.J., Heister, A., van der Kemp, A.W., Knoers, N.V., Hoenderop, J.G., Bindels, R.J., 2009b. A missense mutation in the Kv1.1 voltage-gated potassium channel-encoding gene KCNA1 is linked to human autosomal dominant hypomagnesemia. J. Clin. Invest. 119, 936–942.

Graves, T.D., Rajakulendran, S., Zuberi, S.M., Morris, H.R., Schorge, S., Hanna, M.G., Kullmann, D.M., 2010. Nongenetic factors influence severity of episodic ataxia type 1 in monozygotic twins. Neurology 75, 367–372.

Herson, P.S., Virk, M., Rustay, N.R., Bond, C.T., Crabbe, J.C., Adelman, J.P., Maylie, J., 2003. A mouse model of episodic ataxia type-1. Nat. Neurosci. 6, 378–383.

Imai, Y., Inoue, H., Kataoka, A., Hua-Qin, W., Masuda, M., Ikeda, T., Tsukita, K., Soda, M., Kodama, T., Fuwa, T., Honda, Y., Kaneko, S., Matsumoto, S., Wakamatsu, K., Ito, S., Miura, M., Aosaki, T., Itohara, S., Takahashi, R., 2007. Pael receptor is involved in dopamine metabolism in the nigrostriatal system. Neurosci. Res. 59, 413–425.

Imbrici, P., D'Adamo, M.C., Kullmann, D.M., Pessia, M., 2006. Episodic ataxia type 1 mutations in the KCNA1 gene impair the fast inactivation properties of the human potassium channels

Kv1.4-1.1/Kvbeta1.1 and Kv1.4-1.1/Kvbeta1.2. Eur. J. Neurosci. 24, 3073–3083.
Imbrici, P., Gualandi, F., D'Adamo, M.C., Masieri, M.T., Cudia, P., De Grandis, D., Mannucci, R., Nicoletti, I., Tucker, S.J., Ferlini, A., Pessia, M., 2008. A novel KCNA1 mutation identified in an Italian family affected by episodic ataxia type 1. Neuroscience 157, 577–587.
Imbrici, P., D'Adamo, M.C., Grottesi, A., Biscarini, A., Pessia, M., 2011. Episodic ataxia type 1 mutations affect fast inactivation of K^+ channels by a reduction in either subunit surface expression or affinity for inactivation domain. Am. J. Physiol. Cell Physiol. 300, C1314–C1322.
Johnston, J., Forsythe, I.D., Kopp-Scheinpflug, C., 2010. Going native: voltage-gated potassium channels controlling neuronal excitability. J. Physiol. 588, 3187–3200.
Kinali, M., Jungbluth, H., Eunson, L.H., Sewry, C.A., Manzur, A.Y., Mercuri, E., Hanna, M.G., Muntoni, F., 2004. Expanding the phenotype of potassium channelopathy: severe neuromyotonia and skeletal deformities without prominent Episodic Ataxia. Neuromuscul. Disord. 14, 689–693.
Klein, A., Boltshauser, E., Jen, J., Baloh, R.W., 2004. Episodic ataxia type 1 with distal weakness: a novel manifestation of a potassium channelopathy. Neuropediatrics 35, 147–149.
Knight, M.A., Storey, E., McKinlay Gardner, R.J., Hand, P., Forrest, S.M., 2000. Identification of a novel missense mutation L329I in the episodic ataxia type 1 gene KCNA1—a challenging problem. Hum. Mutat. 16, 374.
Kopp-Scheinpflug, C., Fuchs, K., Lippe, W.R., Tempel, B.L., Rubsamen, R., 2003. Decreased temporal precision of auditory signaling in Kcna1-null mice: an electrophysiological study in vivo. J. Neurosci. 23, 9199–9207.
Lee, H., Wang, H., Jen, J.C., Sabatti, C., Baloh, R.W., Nelson, S.F., 2004. A novel mutation in KCNA1 causes episodic ataxia without myokymia. Hum. Mutat. 24, 536.
Lopantsev, V., Tempel, B.L., Schwartzkroin, P.A., 2003. Hyperexcitability of CA3 pyramidal cells in mice lacking the potassium channel subunit Kv1.1. Epilepsia 44, 1506–1512.
Mashimo, T., Yanagihara, K., Tokuda, S., Voigt, B., Takizawa, A., Nakajima, R., Kato, M., Hirabayashi, M., Kuramoto, T., Serikawa, T., 2008. An ENU-induced mutant archive for gene targeting in rats. Nat. Genet. 40, 514–515.
Mashimo, T., Ohmori, I., Ouchida, M., Ohno, Y., Tsurumi, T., Miki, T., Wakamori, M., Ishihara, S., Yoshida, T., Takizawa, A., Kato, M., Hirabayashi, M., Sasa, M., Mori, Y., Serikawa, T., 2010. A missense mutation of the gene encoding voltage-dependent sodium channel (Nav1.1) confers susceptibility to febrile seizures in rats. J. Neurosci. 30, 5744–5753.
Persson, A.S., Klement, G., Almgren, M., Sahlholm, K., Nilsson, J., Petersson, S., Arhem, P., Schalling, M., Lavebratt, C., 2005. A truncated Kv1.1 protein in the brain of the megencephaly mouse: expression and interaction. BMC Neurosci. 6, 65.
Pessia, M., Hanna, M.G., 1993. Episodic Ataxia Type 1. Vol. In: Pagon, R.A., Bird, T.D., Dolan, C.R., Stephens, K. (Eds.), GeneReviews. University of Washington, Seattle, Seattle WA (Vol.).
Petersson, S., Persson, A.S., Johansen, J.E., Ingvar, M., Nilsson, J., Klement, G., Arhem, P., Schalling, M., Lavebratt, C., 2003. Truncation of the Shaker-like voltage-gated potassium channel, Kv1.1, causes megencephaly. Eur. J. Neurosci. 18, 3231–3240.
Poujois, A., Antoine, J.C., Combes, A., Touraine, R.L., 2006. Chronic neuromyotonia as a phenotypic variation associated with a new mutation in the KCNA1 gene. J. Neurol. 253, 957–959.
Rajakulendran, S., Schorge, S., Kullmann, D.M., Hanna, M.G., 2007. Episodic ataxia type 1: a neuronal potassium channelopathy. Neurotherapeutics 4, 258–266.
Rho, J.M., Szot, P., Tempel, B.L., Schwartzkroin, P.A., 1999. Developmental seizure susceptibility of kv1.1 potassium channel knockout mice. Dev. Neurosci. 21, 320–327.
Scheffer, H., Brunt, E.R., Mol, G.J., van der Vlies, P., Stulp, R.P., Verlind, E., Mantel, G., Averyanov, Y.N., Hofstra, R.M., Buys, C.H., 1998. Three novel KCNA1 mutations in episodic ataxia type I families. Hum. Genet. 102, 464–466.
Schulte, U., Thumfart, J.O., Klocker, N., Sailer, C.A., Bildl, W., Biniossek, M., Dehn, D., Deller, T., Eble, S., Abbass, K., Wangler, T., Knaus, H.G., Fakler, B., 2006. The epilepsy-linked Lgi1 protein assembles into presynaptic Kv1 channels and inhibits inactivation by Kvbeta1. Neuron 49, 697–706.
Shook, S.J., Mamsa, H., Jen, J.C., Baloh, R.W., Zhou, L., 2008. Novel mutation in KCNA1 causes episodic ataxia with paroxysmal dyspnea. Muscle Nerve 37, 399–402.
Smart, S.L., Lopantsev, V., Zhang, C.L., Robbins, C.A., Wang, H., Chiu, S.Y., Schwartzkroin, P.A., Messing, A., Tempel, B.L., 1998. Deletion of the K(V)1.1 potassium channel causes epilepsy in mice. Neuron 20, 809–819.
Tomlinson, S.E., Tan, S.V., Kullmann, D.M., Griggs, R.C., Burke, D., Hanna, M.G., Bostock, H., 2010. Nerve excitability studies characterize Kv1.1 fast potassium channel dysfunction in patients with episodic ataxia type 1. Brain 133, 3530–3540.
Wenzel, H.J., Vacher, H., Clark, E., Trimmer, J.S., Lee, A.L., Sapolsky, R.M., Tempel, B.L., Schwartzkroin, P.A., 2007. Structural consequences of Kcna1 gene deletion and transfer in the mouse hippocampus. Epilepsia 48, 2023–2046.
Wulff, H., Castle, N.A., Pardo, L.A., 2009. Voltage-gated potassium channels as therapeutic targets. Nat. Rev. Drug Discov. 8, 982–1001.
Yoshimi, K., Tanaka, T., Takizawa, A., Kato, M., Hirabayashi, M., Mashimo, T., Serikawa, T., Kuramoto, T., 2009. Enhanced colitis-associated colon carcinogenesis in a novel Apc mutant rat. Cancer Sci. 100, 2022–2027.
Zerr, P., Adelman, J.P., Maylie, J., 1998. Characterization of three episodic ataxia mutations in the human Kv1.1 potassium channel. FEBS Lett. 431, 461–464.
Zhang, C.L., Messing, A., Chiu, S.Y., 1999. Specific alteration of spontaneous GABAergic inhibition in cerebellar purkinje cells in mice lacking the potassium channel Kv1. 1. J. Neurosci. 19, 2852–2864.
Zhou, L., Zhang, C.L., Messing, A., Chiu, S.Y., 1998. Temperature-sensitive neuromuscular transmission in Kv1.1 null mice: role of potassium channels under the myelin sheath in young nerves. J. Neurosci. 18, 7200–7215.
Zuberi, S.M., Eunson, L.H., Spauschus, A., De Silva, R., Tolmie, J., Wood, N.W., McWilliam, R.C., Stephenson, J.B., Kullmann, D.M., Hanna, M.G., 1999. A novel mutation in the human voltage-gated potassium channel gene (Kv1.1) associates with episodic ataxia type 1 and sometimes with partial epilepsy. Brain 122 (Pt 5), 817–825.

⌘ *Author's Choice*

THE JOURNAL OF BIOLOGICAL CHEMISTRY VOL. 287, NO. 8, pp. 5710–5719, February 17, 2012

Role of Novel Rat-specific Fc Receptor in Macrophage Activation Associated with Crescentic Glomerulonephritis*

Received for publication, May 13, 2011, and in revised form, October 27, 2011 Published, JBC Papers in Press, December 19, 2011, DOI 10.1074/jbc.M111.260695

Theresa H. Page[‡], Zelpha D'Souza[§], Satoshi Nakanishi[¶], Tadao Serikawa[¶], Charles D. Pusey[‖], Timothy J. Aitman[§], H. Terence Cook[**], and Jacques Behmoaras[1]**

From the [‡]Kennedy Institute of Rheumatology Division, Imperial College London, London W6 8LH, United Kingdom, the [§]Medical Research Council Clinical Sciences Centre, the [‖]Renal Department, and the [**]Centre for Complement and Inflammation Research Imperial College London, Hammersmith Hospital, W12 0NN London, United Kingdom, and the [¶]Institute of Laboratory Animals, Graduate School of Medicine, Kyoto University, Yoshidakanoe-cho, Sakyo-ku, Kyoto 606-8501, Japan

Background: Fc receptor-mediated macrophage activation is a major cause of glomerular damage in crescentic glomerulonephritis.
Results: We investigated the role of a novel rat Fc receptor, Fcgr3-rs, in human and rat macrophage activation.
Conclusion: We showed that this receptor prevents the cell signaling of its paralogue (Fcgr3).
Significance: These results provide a novel way to inhibit Fc receptor-mediated cell activation in macrophages.

Crescentic glomerulonephritis (Crgn) is a complex disease where the initial insult is often the glomerular deposition of antibodies against intrinsic or deposited antigens in the glomerulus. The role of Fc receptors in the induction and progression of Crgn is increasingly recognized, and our previous studies have shown that copy number variation in Fcgr3 partially explains the genetic susceptibility of the Wistar-Kyoto (WKY) rat to nephrotoxic nephritis, a rat model of Crgn. The Fcgr3-related sequence (Fcgr3-rs) is a novel rat-specific Fc receptor with a cytoplasmic domain 6 amino acids longer than its paralogue, Fcgr3. The Fcgr3-rs gene is deleted from the WKY rat genome, and this deletion is associated with enhanced macrophage activity in this strain. Here, we investigated the mechanism by which the deletion of Fcgr3-rs in the WKY strain leads to increased macrophage activation. By lentivirus-mediated gene delivery, we generated stably transduced U937 cells expressing either Fcgr3-rs or Fcgr3. In these cells, which lack endogenous Fcgr3 receptors, we show that Fcgr3-rs interacts with the common Fc-γ chain but that Fc receptor-mediated phagocytosis and signaling are defective. Furthermore, in primary macrophages, expression of Fcgr3-rs inhibits Fc receptor-mediated functions, because WKY bone marrow-derived macrophages transduced with Fcgr3-rs had significantly reduced phagocytic activity. This inhibitory effect on phagocytosis was mediated by the novel cytoplasmic domain of Fcgr3-rs. These results suggest that Fcgr3-rs may act to inhibit Fcgr3-mediated signaling and phagocytosis and could be considered as a novel mechanism in the modulation of Fc receptor-mediated cell activation in autoimmune diseases.

In crescentic glomerulonephritis, leukocytes, especially monocytes/macrophages, infiltrating the glomerulus play a critical role in the development of the disease by recognizing immunoglobulins and complement factors via cell surface receptors (1). One of the checkpoints regulating the immune response in glomerular inflammation is through leukocyte cell surface receptors for the Fc (fragment crystallizable) portion of IgG. The family of Fc receptors can regulate the fine balance between pro-inflammatory *versus* anti-inflammatory states of cell activation, and there is increasing evidence suggesting that genetic susceptibility to autoimmune diseases is partly dependent on Fc receptor-mediated activating and inhibitory signaling pathways determining the net signal (pro- or anti-inflammatory) in the progression of the disease (2, 3). In systemic lupus erythematosus, aberrant expression or the presence of allelic variants of FcγRs with altered functionality have been reported to contribute to the pathogenesis of the disease (4).

There are two distinct classes of Fc receptors: the activatory and the inhibitory receptors. Most activatory receptors serve as the ligand-binding component of a receptor that also includes a signal transducing molecule containing an immunoreceptor tyrosine-based activation motif (ITAM)[2] (5). In monocytes and macrophages, this role is fulfilled by the common γ chain. Signaling via its ITAM motif triggers the activation of multiple downstream signaling pathways including the activation of Src and Syk kinases, calcium mobilization, and NF-κB activation, leading ultimately to cellular responses such as phagocytosis and cytokine production. The importance of activatory Fcγ receptors in glomerulonephritis has been shown using mice engineered to lack the ITAM-bearing Fc receptor γ chain. We and others have shown that these mice are protected from glomerulonephritis induced by antibodies to glomerular basement membrane (6–8). In contrast, the inhibitory Fc receptor FcγRIIB has an immunoreceptor tyrosine-based inhibitory

* This work was supported by intramural funding from the Wellcome Trust, Clinical Sciences Centre, and the United Kingdom Medical Research Council. Recipient of an Imperial College Junior Research Fellowship.
⌘ *Author's Choice*—Final version full access.
[1] To whom correspondence should be addressed: Centre for Complement and Inflammation Research, Imperial College London, Hammersmith Hospital, Du Cane Rd., W12 0NN London, UK. Tel.: 44-20-8383-2339; Fax: 44-20-8383-8577; E-mail: Jacquesb@imperial.ac.uk.

[2] The abbreviations used are: ITAM, immunoreceptor tyrosine-based activation motif; FcR, Fc receptor; BMDM, bone marrow-derived macrophage; NTN, nephrotoxic nephritis; Crgn, Crescentic glomerulonephritis; WKY, Wistar-Kyoto; qRT, quantitative RT; PMA, phorbol 12-myristate 13-acetate.

motif and does not use the common γ chain (3). Activatory and inhibitory Fcγ receptors are often expressed on the same cell, and when co-aggregated by IgG antibody, the net signal to the cell depends on the sum total of the activator and inhibitor signals, thus setting thresholds for effector cell responses (3).

In our previous studies of nephrotoxic nephritis (NTN), a model of crescentic glomerulonephritis in the Wistar-Kyoto (WKY) rat, we performed genome-wide linkage analysis for glomerular crescents, macrophage infiltration, and proteinuria in an F2 population derived from NTN-susceptible WKY and NTN-resistant Lewis rats (9). The most significant linkage (logarithm of odds > 8) was obtained with a quantitative trait locus mapping to chromosome 13 (*Crgn1*) accounting, respectively, for 21.8, 16.7, and 12.9% of the genetic variance in crescent formation, proteinuria, and macrophage infiltration. Positional cloning of *Crgn1* led to the identification and functional characterization of the *Fcgr3*-related sequence (*Fcgr3-rs*), a novel rat-specific activatory Fc receptor arising from copy number variation in the *Fcgr3* gene (9). The genomic rearrangement in the *Fcgr3* gene is such that there is a duplication of exon 5 in the NTN-resistant Lewis genomic DNA with the presence of a shorter exon lacking a sequence of 226 bp in its 3′-untranslated region. This shorter exon 5 was deleted in the WKY genome, suggesting a copy number variation in the *Fcgr3* gene. Sequence analysis of this shorter copy of exon 5 revealed deletion of a single guanine nucleotide at position 129 (ΔG129) in the coding sequence of the cytoplasmic domain, resulting in a frameshift and generating a novel cytoplasmic domain 6 amino acids longer than that encoded by *Fcgr3*. We designated this copy number variant *Fcgr3*-related sequence (*Fcgr3-rs*) and showed that this novel variant is transcribed and translated in the Lewis strain, whereas it is deleted from the WKY genome (9).

Given the increased macrophage activity and associated NTN susceptibility in the WKY rat that lacks the Fcgr3-rs molecule, it is important to understand how the presence of this molecule might be influencing macrophage activity. Thus, we have studied the role of *Fcgr3-rs* in macrophage activation. We first investigated whether the genomic duplication/deletion event giving rise to *Fcgr3-rs* occurred during the derivation of inbred Wistar-related colonies. We have then generated U937 cells stably expressing either *Fcgr3* or *Fcgr3-rs* and have studied the role of *Fcgr3*-rs in macrophage activation both in U937 cells and WKY bone marrow-derived macrophages (BMDMs) transduced with *Fcgr3-rs*. Our results show that the absence of Fcgr3-rs is not specific to the WKY strain but is widely distributed throughout the rat phylogenetic tree. Furthermore, in both human monocyte cell lines and primary rat macrophages, expression of *Fcgr3-rs* inhibits *Fcgr3*-mediated signaling and phagocytosis, suggesting that the rat possesses a unique mechanism by which Fc receptor-mediated cell activation can be modulated.

EXPERIMENTAL PROCEDURES

Animals—WKY (WKY/NCrl) rats were purchased from Charles River. All of the procedures were performed in accordance with the United Kingdom Animals (Scientific Procedures) Act.

Reagents—RPMI 1640 containing 25 mM L-glutamine was purchased from Biowhittaker (Berkshire, UK). FCS was from PAA (Yeovil, UK) or Labtech (East Sussex, UK). All of the growth media were supplemented with penicillin (100 units/ml) and streptomycin (100 μg/ml), supplied as a 100× sterile solution from Biowhittaker. LPS was obtained from Sigma. Antibodies were from Millipore (anti-Myc), Santa Cruz ($F(ab')_2$, anti-Syk, anti-CD16), GE Healthcare (HRP-conjugated antibodies for Western blot), or Upstate Biotech (anti-γ chain). pCSGW vector was a gift from Richard Jenner (University College London, London, UK).

Fcgr3 Exon 5 Genotyping—*Fcgr3* exon 5 genotype was determined by PCR and agarose gel electrophoresis by using primers to amplify exon 5 genomic DNA from 134 laboratory rat strains and substrains available in the National BioResource project for the rat in Japan. The primer sequence used is as follows: 5′-GTCCCTAAATTCTGAATTTC-3′ and 5′-AAAGAAGTCACAGAAAGGAG-3′.

Lentiviral Constructs—*Fcgr3* and *Fcgr3-rs* were amplified from Lewis spleen cDNA with forward primer 5′-AAGCTTGCCACCATGACTTTGGAG-3′ and reverse primer 5′-TCTAGATTATTAGCCATACGATGGGAT-3′. Clones were reamplified with forward primer 5′-CGGAAGCTTGCCACCATGGAGCAGAAACTCATCTCTGAAGAGGATCTGACTTTGGAGACCCAGATGTTTCAG-3′ and reverse primer 5′-CCTTGAGCACCTGGATCCATGGGG-3′ and recloned. Site-directed mutagenesis was performed on the Fcgr3 construct for ΔG129 with primers 5′-GAGAAATCTTCAAACCTCGGGGAGGACTGGAGGAAATCCC-3′ (forward) and 5′-GGGATTTCCTCCAGTCCTCCCCGAGGTTTGAAGATTTCTC-3′ (reverse). All α subunit constructs were cloned into the pcDNA3.1/Hygro(+) expression vector (Invitrogen). For inserting an N-terminal Myc tag into the *Fcgr3* constructs, 1.0 μg of the *Fcgr3*, *Fcgr3-rs*, and *Fcgr3*-ΔG constructs were amplified with forward primer 5′-CGGAAGCTTGCCACCATGGAGCAGAAACTCATCTCTGAAGAGGATCTGACTTTGGAGACCCAGATGTTTCAG-3′ and reverse primer 5′-CCTTGAGCACCTGGATCCATGGGG-3′. Constructs and PCR products were cut with HindIII and BamHI and ligated to each other. Lentivirus constructs were prepared as follows: DNA was excised from pCDNA3.1 by digestion with HindIII/XbaI, and blunt ends were created using *Pfu* DNA polymerase. This was ligated into a SmaI cut pENTR4.3F. This "in house" modified version of the pENTR4 gateway vector contains a multiple cloning site downstream of a CMV promoter and upstream of an internal ribosome entry sequence, which mediates expression of an enhanced GFP sequence. Inserts in the correct orientation were identified by diagnostic restriction enzyme digests. Subsequent digestion of this vector with SalI and NotI released a DNA "cassette" containing the "gene of interest" internal ribosome entry sequence-EGP sequences. This was then cloned into the pCSGW lentiviral transfer vector (10) following removal of the vectors own GFP sequence.

Lentiviral Production and Titration—Transfer vector (pCSGW), lentiviral mammalian expression vector (envelope, pMD2.G), and packaging vector (psPAX2) were mixed at a ratio of 4:3:1 and used to infect confluent monolayers of 293T17 cells by calcium phosphate precipitation. The medium was replaced

after 16 h. Media containing virus were collected after a subsequent 24 and 48 h of culture. Insoluble debris was removed by centrifugation and sterilized by filtration through 0.2-μ filters. This crude viral supernatant was stored at −80 °C until use. Titers of viral preparations produced in this way were established by infection of U937 cells as follows. Briefly, U937 cells were mixed with varying dilutions of viral supernatant (typically 1/5 to 1/500) in the presence of 8 mg/ml polybrene (hexadimethrine bromide; Sigma). The cells were "spinoculated" by spinning at 2200 rpm for 2 h at 30 °C. After 72 h, the percentage of GFP-positive cells (FITC channel) was determined by FACS analysis (using a LSRII FACS). The lowest dilution factor with GFP+ score of <20% was used to calculate viral titer.

U937 Lentiviral Line Production—Human monoblastic leukemia U937 cells were infected with lentivirus carrying the gene of interest at a ratio of 1:1 (cells:virus) as described above. The cells were then cultured overnight before removal of virus containing media. Cell surface Myc-positive cells (Myc-Fcgr3 or Myc-Fcgr3RS) were isolated by panning on 10-cm Petri dishes coated with anti-Myc antibody (Millipore). Adherent cells were expanded in culture and used in subsequent experiments. GFP-positive cells expressing pCSGW (no surface Myc) were isolated by cell sorting based on FITC fluorescence. Subsequent analysis of cell lines by FACS analysis confirmed 90–100% of cells to be FITC-positive.

FcR Stimulation—The cells were resuspended in ice-cold serum-free RPMI and anti-Myc antibody (Millipore) added to a final concentration of 130 μg/ml. After 60 min of incubation on ice, the cells were washed three times and resuspended in serum free RPMI with 8 mg/ml goat anti-mouse IgGF(ab')$_2$. The cells were then incubated at 37 °C for the indicated times. The reaction was stopped by the addition of gel sample buffer (2% SDS, 10% glycerol, 0.5% β-mercaptoethanol, 50 mM Tris, pH 6.8).

Immunoprecipitations and Western Blot Analysis—The cells were lysed in ice-cold lysis buffer (25 mM Tris, pH 7.6, 150 mM NaCl, 1 mM EDTA, 0.1% Triton X-100, pH 7.8, 1% digitonin), containing protease inhibitor mixture (Sigma) with 1 mM DTT, 10 mM NaF, 100 mM sodium orthovanadate). The nuclei and cell debris were removed by centrifugation, and supernatants were precleared with protein G-Sepharose. Myc-labeled proteins were then precipitated with anti-Myc antibody (Millipore) or isotype matched control antibody and protein G-Sepharose for 1.5 h. Immunoprecipitated complexes were washed in lysis buffer and were resolved on 4–20% SDS-PAGE gels (Criterion).

After electrotransfer on to nitrocellulose membrane, the membranes were blocked in 2% BSA/TBS/Tween (0.05%) and probed with the appropriate antibodies at 4 °C overnight followed by HRP-conjugated secondary antibody. Blots were developed using ECL (Amersham Biosciences).

ELISAs—At 24 h after stimulation, the supernatants were harvested. The concentrations of TNFα and IL-10 were determined by ELISA (PharMingen) according to the manufacturer's instructions. Absorbance was read and analyzed at 450 nm on a spectrophotometric ELISA plate reader (Labsystems Multiskan Biochromic) using the Ascent software program.

BMDM Preparation and Phagocytosis Assay—Femurs from adult WKY rats were isolated and flushed with Hanks' balanced salt solution. Total BM-derived cells were plated and infected with lentivirus carrying the gene of interest at a ratio of 5:1 (cells: virus). 48 h following the infection, the medium was replaced with DMEM that contained 25 mM HEPES (Sigma), 25% L929 conditioned medium, 25% decomplemented FBS (Biosera), penicillin (100 units/ml; Invitrogen), streptomycin (100 μg/ml; Invitrogen), and cultured for 5 days. These cells were characterized as macrophages by ED-1 staining. To assess phagocytosis, latex polystyrene 6.0-μm microspheres (50 beads/macrophage; Polysciences Inc.) were opsonized with BSA-anti-BSA IgG (Sigma) and added to transduced WKY macrophages cultured in 8-well glass chamber slides. Following staining with Diff-Quick fix (Dade Behring), 200 macrophages were counted to determine the number of beads ingested per cell.

Expression Analysis by qRT-PCR—Stably transduced U937 cells were differentiated in macrophages after adding PMA (100 nM) for 48 h and stimulated with LPS (Sigma; 1 μg/ml) for 3 h. Total RNA was extracted using TRIzol (Invitrogen), and one-step qRT-PCR was performed using 100 ng of total RNA and Brilliant II SYBR® Green QRT-PCR Master Mix Kit (Agilent) with specific primers for *Tnfa* and *IL1b1* in an ABI 7900 sequence detection system (Applied Biosystems, Warrington, UK). In rat BMDMs, Fcgr3 levels relative to total Fcgr3 (Fcgr3 + Fcgr3-rs) were assessed by selecting a forward primer where Fcgr3 differs from Fcgr3-rs by two single nucleotide polymorphisms at the end of the 3'-end. The selected primers were Fcgr3-Forward: 5'TCTAGTGTGGTTCCATGCCG-3' and Fcgr3-Reverse: 5'-TGTCCTGTGGAGCCTTGTACT-3'; total Fcgr3 (Fcgr3+Fcgr3-rs)-Forward: 5'-CTCCAGAC-CCCTCAACTGGT-3' and total Fcgr3 (Fcgr3+Fcgr3-rs)-Reverse: 5'-GCAGTAGTAGTTCCCACTGT-3'.

Statistical Analysis—Statistical differences in mean values were compared using one-way analysis of variance followed by Dunnett's multiple comparison post-test; $p < 0.05$ was considered statistically significant.

RESULTS

The Phylogeny of Genomic Deletion of Fcgr3-rs in Laboratory Rat—Exon 5 of *Fcgr3-rs* contains a deletion of a single guanine nucleotide at position 129 (ΔG129) in the coding sequence of the cytoplasmic domain (9). When compared with *Fcgr3*, this ΔG129 variant results in a frameshift in the *Fcgr3-rs* coding sequence and generates a novel cytoplasmic domain 6 amino acids longer than that encoded by *Fcgr3* that was not found in any other species (Fig. 1). We have previously shown that Fcgr3-rs was deleted from NTN-susceptible Kyoto-derived strains (9), but to investigate the distribution of this deletion throughout the rat genealogical tree, we carried out a phylogenetic tree analysis of 94 inbred laboratory strains and 40 of their substrains (Fig. 2). The results show that the deletion of *Fcgr3-rs* is widespread throughout the rat phylogeny (32 of 94 strains), suggesting that the origin of the deletion event is earlier then the derivation of these strains. We also investigated the relative levels of Fcgr3 and Fcgr3-rs mRNA levels in Lewis rat BMDMs by qRT-PCR and showed that although there is relatively

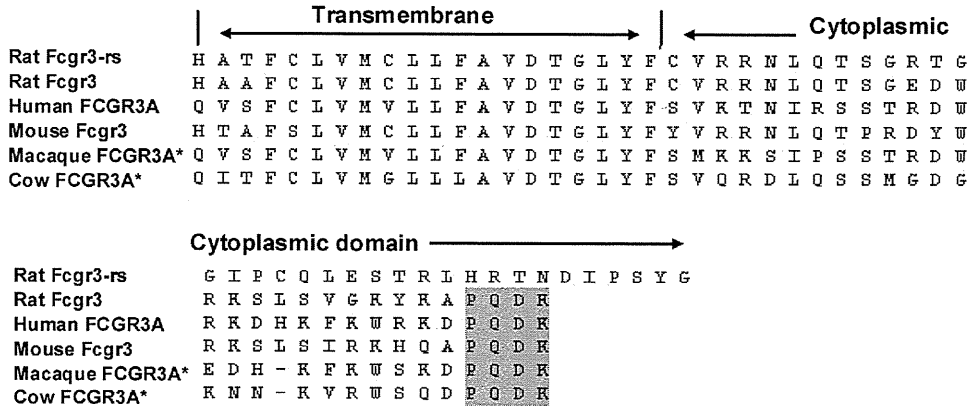

FIGURE 1. **Rat-specific *Fcgr3-rs* is a novel Fc receptor with a unique cytoplasmic domain 6 amino acids longer then *Fcgr3*.** Shown is a comparison of amino acid sequences of transmembrane and cytoplasmic domains of rat *Fcgr3* and *Fcgr3-rs*, human *Fcgr3*, and FCGR3 in other species. Fcgr3-rs has lost the terminal PQDK sequence (*highlighted*) that is highly conserved across species. *, amino acid prediction based on human FCGR3A using Ensembl Genome Browser.

increased Fcgr3 expression when compared with Fcgr3-rs, LPS stimulation did not change the relative levels of both receptors (Table 1).

U937 Cells Expressing Either Fcgr3 or Fcgr3-rs: Surface Expression and Interaction with γ Chain—The U937 cell line does not express any endogenous FcgRIIIA (11) and is therefore an ideal tool for the analysis of FcgRIII receptors, allowing direct functional comparison between the rat orthologues Fcgr3 and Fcgr3-rs. Thus, to study the role of *Fcgr3-rs* in macrophage activation, we generated U937 cells stably transduced with lentivirus constructs expressing the protein of interest. U937 cells were infected with either Myc-tagged Fcgr3 (Myc-Fcgr3), Myc tagged-Fcgr3-rs (Myc-Fcgr3RS), or empty (pCSGW) lentiviral vectors. All of the lentiviral vectors contained GFP. Expression of Myc-Fcgr3 and Myc-Fcgr3-rs was confirmed by fluorescence microscopy, detecting GFP+ cells and also by a Myc Western blot on lysates from stably transduced U937 cells (Fig. 3*A*). We then investigated whether Myc-Fcgr3 and Myc-Fcgr3-rs are expressed on the surface of U937 cells. Flow cytometry analysis using an anti-Myc-APC mouse antibody (mAb) showed that both Myc-Fcgr3 and Myc-Fcgr3-rs are expressed on the cell surface at similar levels in these cells (Fig. 3*B*). Because Fcgr3 transport to and expression at the cell surface is known to be dependent on its association with the common γ chain (12), these findings implied that both the Fcgr3 and Fcgr3-rs molecules were associated with γ chain at the cell surface. Co-immunoprecipitation analysis of U937 cells expressing either Fcgr3 or Fcgr3-rs demonstrated that this was indeed the case (Fig. 3*C*). Thus, although Fcgr3-rs has an additional cytoplasmic domain 6 amino acids longer than its paralogue Fcgr3, it binds the γ-chain on the surface of stably transduced and PMA-differentiated U937 macrophages.

Fcgr3-rs-mediated Signaling and Phagocytosis in U937 Cells—In most macrophage Fc receptor complexes (with the exception of FcgrII), the ITAM-containing common γ-chain is necessary for downstream signaling (13, 14). Thus, the dimeric γ-chain forms multichain complexes with the ligand binding α-chain of Fcgr3 to allow signal transduction (3). This signaling starts with tyrosine phosphorylation of the ITAMs by kinases of the SRC family (15, 16) and leads to the recruitment and subsequent phosphorylation of the Syk kinase, followed by the activation of various downstream targets such as PI3K and NF-κB. Subesquent changes in gene expression led to the induction of inflammatory cytokines such as TNFα. We were therefore keen to understand whether the Fcgr3-rs is able to transduce signals similar to those described for Fcgr3. However, despite its interaction with the γ-chain, cross-linking of Fcgr3-rs with anti-Myc antibody does not lead to phosphorylation of Syk or the degradation of IκBα (Fig. 4*A*). This was not the case for the U937 macrophages stably transduced with Fcgr3 (Fig. 4*A*).

Furthermore, Fc receptor-mediated TNFα production and IgG-opsonized bead phagocytosis were also significantly less in U937 macrophages expressing Fcgr3-rs when compared with U937 macrophages stably transduced with Fcgr3 (Fig. 4*B*). Taken together, these results suggest that the rat-specific Fcgr3-rs is unable to mediate the same intracellular signals as the wild type receptor.

Fcgr3-rs-and TLR4-mediated TNFα and IL-1β Expression Levels—To test whether the relative reduction in TNFα production in U937 cells transduced with Myc-Fcgr3RS is specific to receptor cross-linking, we have stimulated the stably transduced PMA-differentiated U937 cells with LPS for 3 h and measured TNFα and IL-1β expression levels by qRT-PCR (Fig. 5). Although the results have confirmed the previously shown up-regulation of these genes in U937 cells (17), there was no significant difference in the up-regulation of TNFα and IL-1β between U937 + Myc-Fcgr3 and U937 + Myc-Fcgr3RS, demonstrating that the inability of these cells to produce TNFα is not an intrinsic property of these cells and is specific to Fcgr3 stimulation (Fig. 5).

The Role of the Novel Cytoplasmic Domain of Fcgr3-rs in Rat and Human Macrophage Activation—To study the effect of Fcgr3-rs on the phagocytic activity of primary WKY BMDMs where other endogenous, FcRs (Fcgr3 and others) are expressed, we transduced these cells with lentivirus encoding either Myc-Fcgr3rs or Myc-Fcgr3 and used cells transduced with the empty vector (pCSGW) as controls.

Because the Fcgr3-rs also contains a number of single-base pair substitutions in its extracellular domain, we were also keen to establish whether these might explain the differences between the related sequence and wild type Fcgr3 molecules, possibly as a

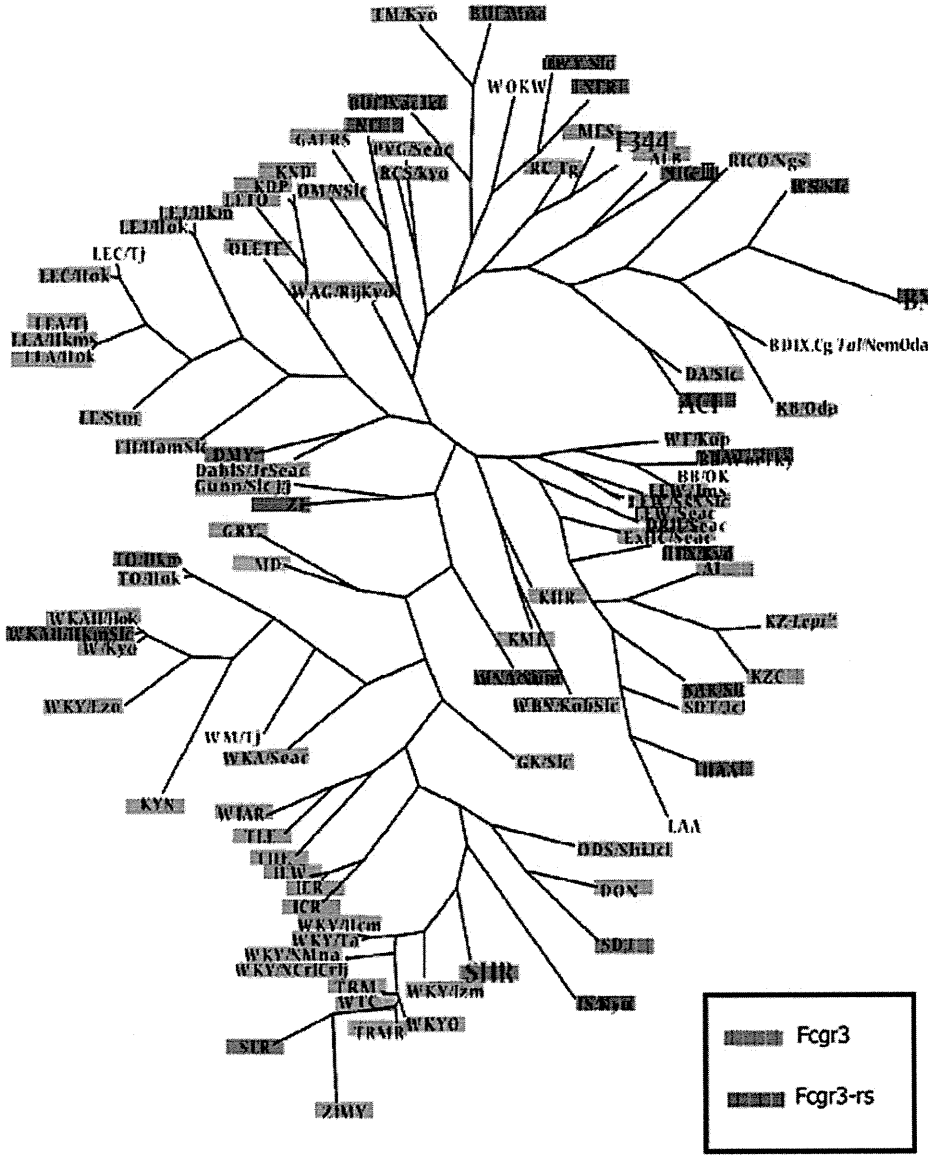

FIGURE 2. **Phylogenetic tree of 134 laboratory rat strains according to the presence or absence of *Fcgr3-rs* in the genome.** A phylogenetic tree of 94 strains is shown. Strains having numerous substrains (*i.e.* SHR, F344) are shown in capital letters, and all of the substrains showed the same genotype as the founder strain. The tree was developed through a heuristic search for maximum parsimony implemented in PAUP 4.0b10. TreeView was used to display the radial tree. For BD IX, LEC/Tj, and WM/Tj, genotypes could not be determined.

TABLE 1

Relative mRNA levels of Fcgr3 and Fcgr3-rs in Lewis rat BMDMs

Expression was assessed by qRT-PCR with specific primers that differentiate between Fcgr3 and Fcgr3-rs in basal and LPS-stimulated (100 ng/ml, for 5 h) BMDMs. Fcgr3 and Fcgr3-rs expression levels were normalized to total Fcgr3 (Fcgr3 + Fcgr3-rs) levels.

	BMDM	
Expression	Basal	LPS
Fcgr3/(Fcgr3 + Fcgr3-rs)	0.73 ± 0.02	0.67 ± 0.01
Fcgr3-rs/(Fcgr3 + Fcgr3-rs)	0.27 ± 0.02	0.33 ± 0.01

result of altered FcR binding. Thus, we also generated an additional lentiviral construct encoding a chimeric protein to specifically test the effect of the novel cytoplasmic domain of Fcgr3-rs on Fc receptor-mediated phagocytosis. Fcgr3-ΔG contains the wild type Fcgr3 extracellular, transmembrane, and cytoplasmic domains with the presence of the Fcgr3-rs-specific novel cytoplasmic domain (9) (Fig. 6*A*).

We first measured the expression of Fcgr3 by using primers specific for the transmembrane domain, thereby allowing differential amplification between *Fcgr3* and *Fcgr3-rs* transcripts (Fig. 6*B*). We then measured the number of opsonized beads phagocytosed by 200 WKY BMDMs transduced with each different lentiviral construct.

Phagocytosis was significantly reduced in Fcgr3-rs transduced WKY BMDMs when compared with those transduced with pCSGW (Fig. 6*C*). This inhibitory effect is clearly mediated by the novel cytoplasmic domain of Fcgr3-rs, because similar reductions in phagocytic activity were seen in WKY BMDMs transduced either with Fcgr3-ΔG or with Fcgr3-rs (Fig. 6*C*). Taken together, these data suggest that the presence of FcRs containing the related sequence cytoplasmic domain is able to reduce phagocytosis mediated by endogenous FcRs in the WKY BMDMs.

To further understand the mechanism of action of the Fcgr3-rs, we then investigated how the Fcgr3 and Fcgr3-rs

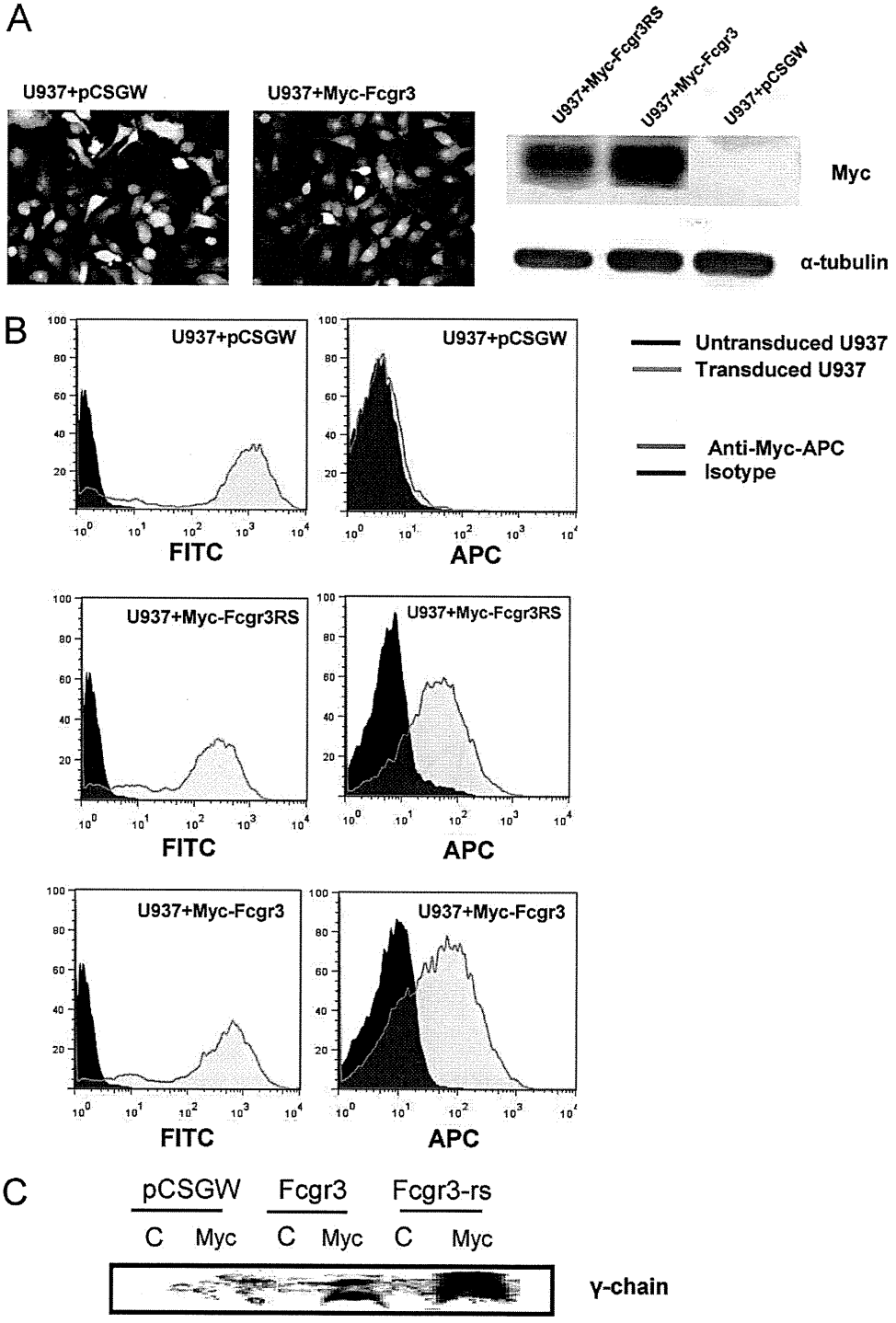

FIGURE 3. **Surface expression of Fcgr3-rs and Fcgr3 and assessment of their interaction with the γ chain in stably transduced U937 cells.** *A*, illustration of GFP expression in U937 + pCSGW and U937 + Myc-Fcgr3 by fluorescent microscopy (×40). Myc and α-tubulin (loading control) Western blots of whole cell lysates from stably transduced U937 cells are shown. *B*, the human monoblastic leukemia cell line U937 was stably transduced to express either Myc-Fcgr3 (U937 + Myc-Fcgr3) or Myc-Fcgr3RS (U937 + Myc-Fcgr3RS) lentiviral constructs co-expressing GFP together with transgene. Untransduced cells (U937) and cells transduced with lentiviral construct expressing GFP alone (without any transgene, U937 + pCSGW) were used as controls. Surface expression was measured by using anti-Myc-APC mAb. All of the transduced cells were GFP+ as shown by FITC emission. *C*, stably transduced U937 cells were differentiated into macrophages after adding PMA (100 nM) for 48 h, and cell lysates were precipitated with anti-Myc antibody. Immunoprecipitated proteins were blotted with anti-γ chain antibody.

interact with TLR4-mediated TNFα production following LPS stimulation. U937 cells transduced with FcRs (U937 + Myc-Fcgr3, U937 + MycFcgr3RS, and U937 + Myc-Fcgr3ΔG) were cross-linked with anti-Myc antibodies and IgG F(ab′)$_2$. Following washing, the cells were stimulated with LPS for 5 h. TNFα and IL-10 protein levels were measured by sandwich ELISA.

In the absence of any additional FcR expression in these cells, treatment with Ab·Fab complexes resulted in a 38% decrease in TNF production. This was further decreased in

the presence of the Fcgr3 molecule to 50% of that seen in cells that are not cross-linked, revealing that signals from Fcgr3 act to reduce TLR4-induced TNF production in U937 cells (Fig. 6*D*). In contrast, the presence of either the Fcgr3-rs or Fcgr3ΔG did not result in any changes in TNFα production compared with cells that are not cross-linked. Levels of IL-10 produced in these cells did not differ significantly between Fcgr3 and FcgR3-rs or FcgR3-ΔG cells (Fig. 6*E*), revealing that the Fcgr3-rs is not functioning in these cells by increasing levels of this anti-inflammatory cytokine.

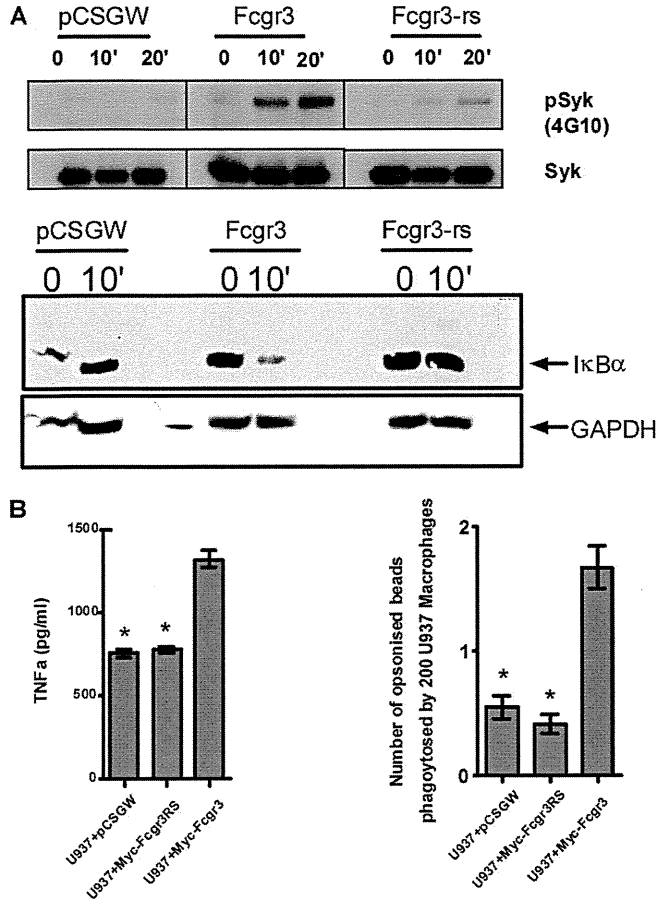

FIGURE 4. **Fc receptor-mediated signaling and phagocytosis in U937 cells stably transduced with Myc-Fcgr3RS.** *A*, Fc receptor stimulation after cross-linking with anti-Myc Ab for a maximum of 20 min and analysis of Syk phosphorylation and IκBα degradation in stably transduced U937-derived macrophages. *B*, TNFα levels were assessed by sandwich ELISA after cross-linking stably transduced U937 macrophages by anti-Myc mAb. Supernatants were collected after 48 h of incubation. Fc receptor-mediated bead phagocytosis was assayed by incubating macrophages with IgG opsonized latex beads. Nonopsonized beads did not show any phagocytosis. *, $p < 0.001$ when compared with U937 + Myc-Fcgr3.

DISCUSSION

There is considerable evidence from experimental models of crescentic glomerulonephritis that Fcγ receptors play a central role in disease progression. In mice, the FcR chain-deficient mice ($FcR\gamma^{-/-}$) lack surface expression of both murine activator Fc receptors I, III, and IV, and the high affinity IgE receptor (FcRI) (18). Several studies have shown that $FcR\gamma^{-/-}$ mice are protected from disease in accelerated nephrotoxic nephritis (6, 7, 19), and we have shown that the disease is mediated by Fcγ receptors on circulating leukocytes and not intrinsic renal cells (8). Our previous studies in the NTN model in the Wistar Kyoto rat showed that the disease architecture is complex and highly heritable, with seven quantitative trait loci (*Crgn1–7*) linked to the percentage of glomerular crescents and controlling mainly macrophage activation through distinct transcriptome profiles (9, 20–22). In this model, we showed that copy number variation in rat *Fcgr3* locus led to the deletion of *Fcgr3-rs* in the WKY rat, predisposing this strain to enhanced macrophage activity (9).

The purpose of the current study was to understand the mechanism by which the genomic deletion of *Fcgr3-rs* leads to macrophage overactivation and whether the novel cytoplasmic domain binds to the common γ chain to trigger downstream signaling pathways. We first investigated the distribution of *Fcgr3-rs* deletion throughout the rat phylogeny and found that the deletion was widespread. It was previously reported that five outbred Wistar and one Long-Evans stocks have Fcgr3-rs (23), suggesting that the deletion has originated from the ancestor outbred Wistar colony in the Wistar institute in the United States. We now confirm and extend these findings because all of the laboratory rat strains that we genotyped for Fcgr3 copy

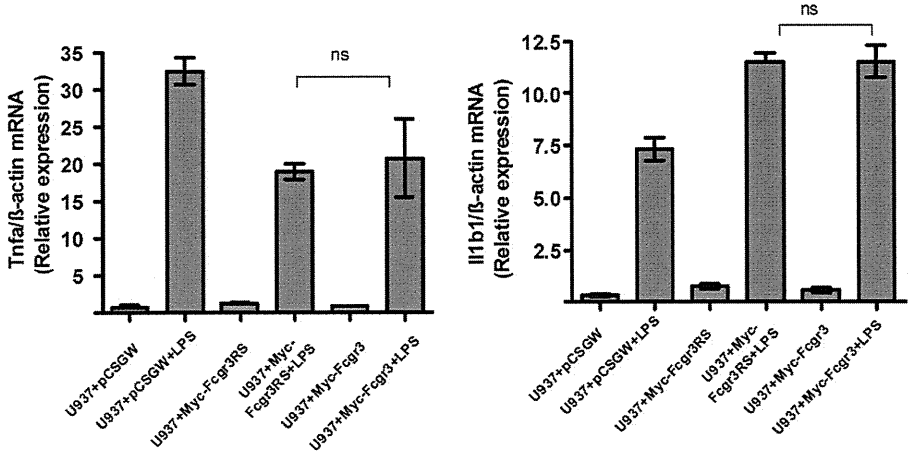

FIGURE 5. **Fcgr3-rs does not affect TLR4-mediated *Tnfa* and *Il1b1* expressions in stably transduced U937 cells.** Stably transduced U937 cells were differentiated in macrophages after adding PMA (100 nM) for 48 h and stimulated with LPS (1 μg/ml) for 3 h. *Tnfa* and *Il1b1* gene expression were measured by qRT-PCR. *ns*, not significant.

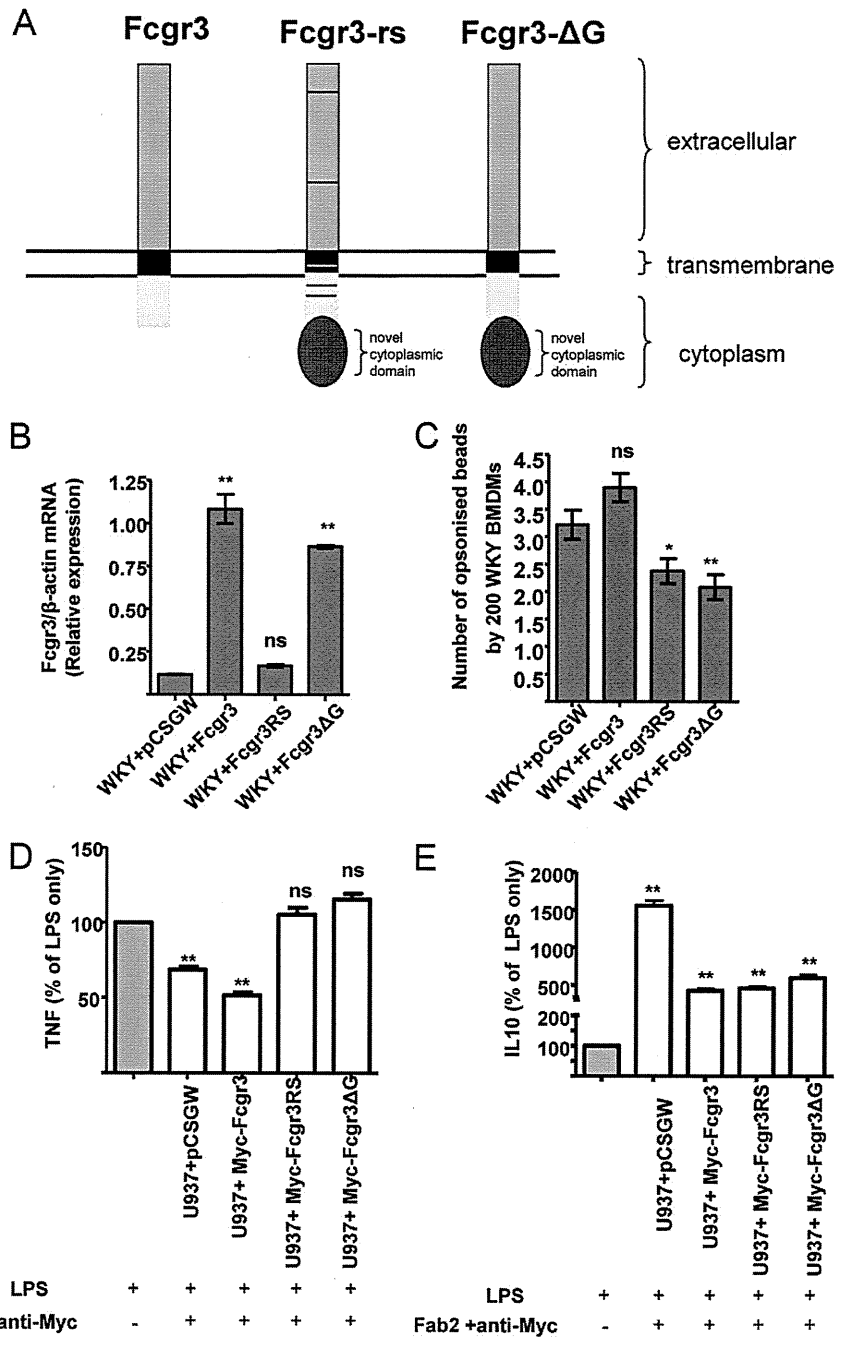

FIGURE 6. **Fcgr3-rs inhibits Fc receptor-mediated phagocytosis in WKY BMDMs.** *A*, schematic representation of the functional differences between Fcgr3 and Fcgr3-rs. Although there are amino acid changes in the Fcgr3-rs extracellular, transmembrane, and cytoplasmic domains (indicated by *bars*) when compared with Fcgr3, the major structural difference is the presence of a novel cytoplasmic domain. The chimeric Fcgr3-ΔG has the extracellular transmembrane and cytoplasmic domains identical to Fcgr3, the only difference being the presence of the novel cytoplasmic domain. *B*, *Fcgr3* expression was assessed by qRT-PCR in stably transduced U937 cells by using specific primers designed based on polymorphisms in the transmembrane domain differentiating between *Fcgr3* and *Fcgr3-rs*. The expression of Myc-Fcgr3 ΔG was also assessed and showed similar expression levels as Fcgr3. This is because Fcgr3 and Fcgr3-ΔG share the same sequence in the transmembrane domain. *C*, WKY bone marrow-derived cells were transduced with lentiviral constructs co-expressing GFP with either Myc-tagged Fcgr3-rs (Myc-Fcgr3RS) or Myc-tagged wild type Fcgr3 (Myc-Fcgr3) or Myc-tagged Fcgr3-ΔG. The lentiviral construct expressing GFP alone (without any transgene) was used as control (pCSGW). The cells were then differentiated into BM-derived macrophages by culturing in DMEM containing L929, and Fc receptor-mediated phagocytosis was performed. **, $p < 0.01$; *, $p < 0.05$; *ns*, not significant when compared with pCSGW. *D* and *E*, LPS-induced TNFα (*D*) and IL-10 (*E*) levels were assessed by sandwich ELISA after cross-linking stably transduced U937 macrophages by anti-Myc mAb and F(ab′)$_2$. Following cross-linking, the cells were washed, and supernatants were collected after 5 h of incubation with LPS (1 μg/ml). TNFα and IL-10 production were expressed as a percentage of that produced in LPS-stimulated cells without FcR cross-linking (100% of cytokine production). **, $p < 0.001$ when compared with LPS-stimulated cells without FcR cross-linking (100% of cytokine production; histogram in *gray*)

number variation are derived from outbred Wistar and Long-Evans stocks.

Previously, to investigate how Fcgr3-rs exerts its inhibitory effect on Fcγ receptor signaling, we have transfected COS7 cells and have shown that although Fcgr3-rs is expressed on the cell surface, it is less efficient than Fcgr3 in mediating phagocytosis (9). It also had an inhibitory effect on Fcgr3-mediated phagocytosis when both receptors were co-transfected in COS7 cells

(9). However, the COS7 cells are not primarily phagocytic cells and do not endogenously express the γ chain, making it difficult to draw mechanistic conclusions concerning the role of Fcgr3-rs in Fc receptor-mediated signaling and activation. Here we have examined the signaling function of Fcgr3-rs in a human monocyte cell line U937, a well characterized cell line previously used to study Fc receptor function (11). U937 cells constitutively express only Fcgr1 and Fcgr2a but not Fcgr3 (11). We have used lentivirus-mediated gene transfer to generate stably transduced U937 cell lines. Our results showed that Fcgr3-rs associates with the common γ-chain in these cells, but Fc receptor-mediated signaling and phagocytosis are defective. Importantly, WKY BMDMs transduced with the Fcgr3-rs also showed reduced bead phagocytosis, and this was mediated through the rat-specific novel cytoplasmic domain.

It is well established that the transmembrane domain is required for association with the γ chain and consequently cell surface expression of Fcgr3 (24). Because of the amino acid changes between Fcgr3 and Fcgr3-rs in the transmembrane domains, it could therefore be argued that the amino acid changes simply prevented *Fcgr3-rs* expression. This, however, was not the case, and in both U937 cells and primary rat macrophages, Fcgr3-rs was expressed at the cell surface at similar levels to Fcgr3. The use of the ΔG chimeric molecule, which contains the extracellular and transmembrane domains of Fcgr3 combined with the cytoplasmic domain of Fcgr3-rs, also demonstrates that the differences seen between Fcgr3 and Fcgr3-rs functions are mediated only by the novel cytoplasmic domain of Fcgr3-rs and cannot be explained by point mutations in the extracellular domain of Fcgr3-rs, which might simply have prevented Fc binding of IgG.

The majority of signaling cascades emanating from the Fcgr3 receptor complex are thought to be derived from the γ chain via its ITAM motifs. Thus, removal of the γ chain cytoplasmic domain or mutations of tyrosine residues within the ITAM motifs affects intracellular Ca^{+} levels, PI3K activity and receptor-induced phosphorylation events (25). In particular there is compelling evidence that activation of Syk is essential for subsequent events such as receptor-induced phagocytosis (26, 27). However, the cytoplasmic tail of the Fcgr3 molecule is unlikely to be completely redundant in this process, and Hou *et al.* (28) have suggested that sequences within the cytoplasmic domain of Fcgr3, in particular those close to the transmembrane domain, are required for signaling. Our findings demonstrate that signaling from the Fcgr3-rs is clearly different from that mediated by Fcgr3, because Fcgr3-rs·γ chain complexes do not generate phosphorylated Syk molecules or activate the NF-κB transcription factor that is required for transcription of Fc-responsive genes such as TNFα. Accordingly, IgG-induced TNFα production and phagocytosis are both significantly lower in U937 cells expressing Fcgr3-rs compared with Fcgr3. Moreover, expressing Fcgr3-rs in primary rat WKY BMDMs resulted in lower levels of phagocytosis than cells expressing Fcgr3 alone, suggesting that Fcgr3-rs has an inhibitory effect on Fcgr3-mediated phagocytosis in these cells.

Although the Fcgr3-rs cytoplasmic domain includes a novel sequence with a single tyrosine molecule, this is not an immunoreceptor tyrosine-based inhibitory motif in the same way as that found in the FcgrIIb receptor. Elegant studies by Kim *et al.* (29) have shown that specific regions of the transmembrane region of Fcγ receptors are important for signaling leading to phagocytosis. The same group has provided further evidence on differences in the signaling properties of FcγR1/γ and FcγRIIA such as their interaction with Syk and Src-related tyrosine kinases (30). The region of the cytoplasmic domain shown by Hou *et al.* (28) to be important in signaling is present in the Fcgr3-rs; however, it is possible that the altered sequence of the remainder of the cytoplasmic domain may render this region inaccessible to essential downstream signaling molecules, thereby rendering it inactive. The question of whether the Fcgr3-rs exerts its effects by acting as a decoy receptor, binding immunoglobulins, but not signaling, or whether its novel cytoplasmic domain induces distinct signaling pathways that act to inhibit those from the wt Fcgr3 is therefore an interesting one.

Our demonstration herein that the -rs does not induce Syk or NF-κB activation suggests that this molecule may not signal, and this is underscored by the demonstration that LPS-induced TNF and IL-10 production is unaffected in U937 cells by the presence of the -rs. Taken together, these data add further weight to the argument that Fcgr3-rs is a decoy receptor that is able to bind Fc but unable to signal such that its expression inhibits co-expressed Fc receptor-mediated signaling and cell activation. However, we cannot completely rule out a potential additional role of this receptor, which will lead to inhibition by a novel negative signaling pathway. Investigations into this question are continuing in this laboratory.

In conclusion, our results suggest that the rat-specific *Fcgr3-rs* acts to inhibit *Fcgr3*-mediated signaling and phagocytosis in both rodent and human cells and could be considered as a novel therapeutic mechanism for the modulation of Fc receptor-mediated cell activation in macrophage-mediated diseases such as crescentic glomerulonephritis.

Acknowledgments—We thank Sunil Modi for technical assistance. We are thankful to the National BioResource Project for providing rat strains.

REFERENCES

1. Mason, J. C., and Pusey, C. D. (2008) *The Kidney in Systemic Autoimmune Diseases*, 1st Ed., Elsevier, Amsterdam
2. Nimmerjahn, F., and Ravetch, J. V. (2007) Fc-receptors as regulators of immunity. *Adv. Immunol.* **96,** 179–204
3. Nimmerjahn, F., and Ravetch, J. V. (2008) Fcγ receptors as regulators of immune responses. *Nat. Rev. Immunol.* **8,** 34–47
4. Brown, E. E., Edberg, J. C., and Kimberly, R. P. (2007) Fc receptor genes and the systemic lupus erythematosus diathesis. *Autoimmunity* **40,** 567–581
5. Strzelecka, A., Kwiatkowska, K., and Sobota, A. (1997) Tyrosine phosphorylation and Fcγ receptor-mediated phagocytosis. *FEBS Lett.* **400,** 11–14
6. Park, S. Y., Ueda, S., Ohno, H., Hamano, Y., Tanaka, M., Shiratori, T., Yamazaki, T., Arase, H., Arase, N., Karasawa, A., Sato, S., Ledermann, B., Kondo, Y., Okumura, K., Ra, C., and Saito, T. (1998) Resistance of Fc receptor-deficient mice to fatal glomerulonephritis. *J. Clin. Invest.* **102,** 1229–1238
7. Suzuki, Y., Shirato, I., Okumura, K., Ravetch, J. V., Takai, T., Tomino, Y., and Ra, C. (1998) Distinct contribution of Fc receptors and angiotensin II-dependent pathways in anti-GBM glomerulonephritis. *Kidney Int.* **54,** 1166–1174
8. Tarzi, R. M., Davies, K. A., Robson, M. G., Fossati-Jimack, L., Saito, T.,

Walport, M. J., and Cook, H. T. (2002) Nephrotoxic nephritis is mediated by Fcγ receptors on circulating leukocytes and not intrinsic renal cells. *Kidney Int.* **62,** 2087–2096
9. Aitman, T. J., Dong, R., Vyse, T. J., Norsworthy, P. J., Johnson, M. D., Smith, J., Mangion, J., Roberton-Lowe, C., Marshall, A. J., Petretto, E., Hodges, M. D., Bhangal, G., Patel, S. G., Sheehan-Rooney, K., Duda, M., Cook, P. R., Evans, D. J., Domin, J., Flint, J., Boyle, J. J., Pusey, C. D., and Cook, H. T. (2006) Copy number polymorphism in Fcgr3 predisposes to glomerulonephritis in rats and humans. *Nature* **439,** 851–855
10. Bainbridge, J. W., Stephens, C., Parsley, K., Demaison, C., Halfyard, A., Thrasher, A. J., and Ali, R. R. (2001) *In vivo* gene transfer to the mouse eye using an HIV-based lentiviral vector. Efficient long-term transduction of corneal endothelium and retinal pigment epithelium. *Gene Ther.* **8,** 1665–1668
11. Floto, R. A., Clatworthy, M. R., Heilbronn, K. R., Rosner, D. R., MacAry, P. A., Rankin, A., Lehner, P. J., Ouwehand, W. H., Allen, J. M., Watkins, N. A., and Smith, K. G. (2005) Loss of function of a lupus-associated FcγRIIb polymorphism through exclusion from lipid rafts. *Nat. Med.* **11,** 1056–1058
12. Park, J. G., Isaacs, R. E., Chien, P., and Schreiber, A. D. (1993) In the absence of other Fc receptors, Fc γ RIIIA transmits a phagocytic signal that requires the cytoplasmic domain of its γ subunit. *J. Clin. Invest.* **92,** 1967–1973
13. Lowry, M. B., Duchemin, A. M., Robinson, J. M., and Anderson, C. L. (1998) Functional separation of pseudopod extension and particle internalization during Fc γ receptor-mediated phagocytosis. *J. Exp. Med.* **187,** 161–176
14. Davis, W., Harrison, P. T., Hutchinson, M. J., and Allen, J. M. (1995) Two distinct regions of FC γ RI initiate separate signalling pathways involved in endocytosis and phagocytosis. *EMBO J.* **14,** 432–441
15. Ghazizadeh, S., Bolen, J. B., and Fleit, H. B. (1994) Physical and functional association of Src-related protein tyrosine kinases with Fc γ RII in monocytic THP-1 cells. *J. Biol. Chem.* **269,** 8878–8884
16. Wang, A. V., Scholl, P. R., and Geha, R. S. (1994) Physical and functional association of the high affinity immunoglobulin G receptor (Fc γ RI) with the kinases Hck and Lyn. *J. Exp. Med.* **180,** 1165–1170
17. Sharif, O., Bolshakov, V. N., Raines, S., Newham, P., and Perkins, N. D. (2007) Transcriptional profiling of the LPS induced NF-κB response in macrophages. *BMC Immunol.* **8,** 1
18. Takai, T., Li, M., Sylvestre, D., Clynes, R., and Ravetch, J. V. (1994) FcR γ chain deletion results in pleiotrophic effector cell defects. *Cell* **76,** 519–529
19. Wakayama, H., Hasegawa, Y., Kawabe, T., Hara, T., Matsuo, S., Mizuno, M., Takai, T., Kikutani, H., and Shimokata, K. (2000) Abolition of anti-glomerular basement membrane antibody-mediated glomerulonephritis in FcRγ-deficient mice. *Eur. J. Immunol.* **30,** 1182–1190
20. Behmoaras, J., Bhangal, G., Smith, J., McDonald, K., Mutch, B., Lai, P. C., Domin, J., Game, L., Salama, A., Foxwell, B. M., Pusey, C. D., Cook, H. T., and Aitman, T. J. (2008) Jund is a determinant of macrophage activation and is associated with glomerulonephritis susceptibility. *Nat. Genet.* **40,** 553–559
21. Behmoaras, J., Smith, J., D'Souza, Z., Bhangal, G., Chawanasuntoropoj, R., Tam, F. W., Pusey, C. D., Aitman, T. J., and Cook, H. T. (2010) Genetic loci modulate macrophage activity and glomerular damage in experimental glomerulonephritis. *J. Am. Soc. Nephrol.* **21,** 1136–1144
22. Maratou, K., Behmoaras, J., Fewings, C., Srivastava, P., D'Souza, Z., Smith, J., Game, L., Cook, T., and Aitman, T. (2011) Characterization of the macrophage transcriptome in glomerulonephritis-susceptible and -resistant rat strains. *Genes Immun.* **12,** 78–89
23. Kuramoto, T., Nakanishi, S., and Serikawa, T. (2008) Functional polymorphisms in inbred rat strains and their allele frequencies in commercially available outbred stocks. *Physiol. Genomics* **33,** 205–211
24. Lanier, L. L., Yu, G., and Phillips, J. H. (1991) Analysis of Fc γ RIII (CD16) membrane expression and association with CD3 ζ and Fc epsilon RI-γ by site-directed mutation. *J. Immunol.* **146,** 1571–1576
25. Indik, Z. K., Park, J. G., Hunter, S., and Schreiber, A. D. (1995) The molecular dissection of Fc γ receptor mediated phagocytosis. *Blood* **86,** 4389–4399
26. Crowley, M. T., Costello, P. S., Fitzer-Attas, C. J., Turner, M., Meng, F., Lowell, C., Tybulewicz, V. L., and DeFranco, A. L. (1997) A critical role for Syk in signal transduction and phagocytosis mediated by Fcγ receptors on macrophages. *J. Exp. Med.* **186,** 1027–1039
27. Wirthmueller, U., Kurosaki, T., Murakami, M. S., and Ravetch, J. V. (1992) Signal transduction by Fc γ RIII (CD16) is mediated through the γ chain. *J. Exp. Med.* **175,** 1381–1390
28. Hou, X., Dietrich, J., and Geisler, N. O. (1996) The cytoplasmic tail of FcγRIIIAα is involved in signaling by the low affinity receptor for immunoglobulin G. *J. Biol. Chem.* **271,** 22815–22822
29. Kim, M. K., Huang, Z. Y., Hwang, P. H., Jones, B. A., Sato, N., Hunter, S., Kim-Han, T. H., Worth, R. G., Indik, Z. K., and Schreiber, A. D. (2003) Fcγ receptor transmembrane domains: role in cell surface expression, γ chain interaction, and phagocytosis. *Blood* **101,** 4479–4484
30. Huang, Z. Y., Hunter, S., Kim, M. K., Chien, P., Worth, R. G., Indik, Z. K., and Schreiber, A. D. (2004) The monocyte Fcγ receptors FcγRI/γ and FcγRIIA differ in their interaction with Syk and with Src-related tyrosine kinases. *J. Leukoc. Biol.* **76,** 491–499

厚生労働科学研究費補助金（創薬基盤推進研究事業）
新規遺伝子変異ラット作製技術に基づく生活習慣病・難治性疾患モデルラットの開発
総合研究報告書

発行者　厚生労働科学研究費補助金（創薬基盤推進研究事業）
新規遺伝子変異ラット作製技術に基づく生活習慣病・難治性疾患モデルラットの開発
研究代表者　　中尾　一和

連絡先：〒606-8507　京都市左京区聖護院川原町
京都大学大学院医学研究科　内分泌代謝内科
TEL：075-751-3168